ACIDIC LAMININ: MOLECULAR MECHANISMS AND POTENTIAL FOR NERVOUS TISSUE REPAIR

by

Agnes Elizabeth Haggerty

Bachelor of Science, University of Pittsburgh, 2004

Submitted to the Graduate Faculty of

Swanson School of Engineering in partial fulfillment

of the requirements for the degree of

Doctor of Philosophy

University of Pittsburgh

2014

UNIVERSITY OF PITTSBURGH

SWANSON SCHOOL OF ENGINEERING

This dissertation was presented

by

Agnes Elizabeth Haggerty

It was defended on

November 11, 2014

and approved by

Xinyan Tracy Cui, PhD, Associate Professor, Department of Bioengineering

Adam W. Feinberg, PhD, Assistant Professor, Department of Biomedical Engineering,
Carnegie Mellon University

Yadong Wang, PhD, Professor, Department of Bioengineering

Dissertation Director: Martin Oudega, PhD, Assistant Professor, Department of Physical
Medicine and Rehabilitation

**ACIDIC LAMININ: MOLECULAR MECHANISMS AND POTENTIAL
FOR NERVOUS TISSUE REPAIR**

Agnes E. Haggerty, PhD

University of Pittsburgh, 2014

Biomaterials have shown promise for treatment of injuries to the nervous system. Laminin, a glycoprotein, forms distinct polymers under neutral (pH 7; neutral laminin, nLam) or acidic (pH 4; acidic laminin, aLam) conditions (1, 2). aLam promotes significant axonal growth (2), making it of interest as a therapeutic for nervous tissue injuries.

In this thesis, instead of as a substrate, we evaluate unbound aLam. In Chapter 2.1, we use an *in vitro* model system to investigate the mechanisms underlying aLam growth promotion. Results indicate: 1) laminin can act as a signaling molecule promoting outgrowth of adult neurons *in vitro*; 2) aLam is a more efficient promoter of outgrowth than nLam; 3) both polymers signal through α1 and α3 integrins without increasing their expression; 4) aLam, increases α3 integrins when α1 integrins are blocked; 6) aLam increases vinculin, a focal adhesion complex protein. These findings indicate that aLam promotes outgrowth by increasing integrin activation to enhance neurite outgrowth.

In Chapter 2.2 microcontact printing and live imaging were combined to evaluate aLam's effects on growth dynamics. Our results suggest: 1) neurons will adhere to stamps and grow in a directional manner in culture; 2) cells did not adhere or grow well during live imaging. Results indicate potential for directing neuronal outgrowth, but optimization is necessary to assess growth dynamics.

Peripheral nerve injury (PNI) and spinal cord injury (SCI) are devastating. In Chapter 3.1 we investigate aLam's treatment potential in PNI. R esults indicate that aLam treatment: 1) increased presence of larger diameter axons; 2) facilitated compliance in treadmill walking; 3) alleviated autophagia; 4) did not affect motor function, axon number or myelination. These data show that aLam treatment elicits an axon growth response without affecting motor function recovery. Further research is needed to optimize treatment for functional improvements.

Chapter 3.2 evaluates aLam treatment after SCI. Results show that aLam treatment: 1) did not affect axon regeneration; 2) decreased astrocyte activation; 3) did not affect neuropathic pain or motor outcomes. The data indicate treatment did not lead to functional improvements. Further research is needed to investigate the potential of aLam for SCI repair.

TABLE OF CONTENTS

LIST OF TABLES

LIST OF FIGURES

PREFACE

Many people have provided essential support in order for this thesis to be realized. Primarily, I have to thank my daughter, Kaila, my inspiration, whose enthusiasm about my research and unfailing belief in me and my love of science, has rekindled in me a passion and energy that at times was in danger of burning low.

Many thanks and limitless gratitude to my mentor, Martin Oudega, who gave me the opportunity to work in his lab and has been patient in teaching both laboratory and life skills and for creating an amazing environment in which to work and learn; to my committee, Tracy Cui, Yadong Wang and Adam Feinberg who have donated their time, expertise, and at times their lab equipment and personnel to bring this to fruition; to Katarina Vajn, Gaby Ritfeld, Tabitha Novosat and the past and current members of the Spinal Cord Repair Lab; to all of the staff and faculty of the Center for Biological Imaging, especially Doris Clay and Callen Wallace, the CBI is full of remarkable personnel who have provided many answers to my many questions and allowed me to use their remarkable equipment; to the PICAN lab and collaborators who started me on t his great journey; and lastly to my family, both born and chosen, you've always supported, encouraged and challenged me and there is no question that I succeed where others have failed not due to my own unique abilities or drive, but because of my extraordinary support group.

1.0   INTRODUCTION

Spinal cord injury (SCI) and peripheral nerve injury (PNI) lead to loss of motor and sensory function. Motor vehicle accidents have historically been a main cause of these types of nervous tissue trauma. In recent years in the United States, neuropathies due to diabetes has increasingly contributed to the overall number of people with PNI-related functional impairments (3). The spinal cord contains long descending motor axons originating from neurons in various brain nuclei. The peripheral nerves contain long motor and/or sensory axons from neurons in the ventral spinal cord and dorsal root ganglia, respectively. Trauma to these anatomical structures typically severs these axonal tracts thereby disrupting the information to and from the target cells. Neuronal death due to an injury to the spinal cord and peripheral nerve is relatively limited because of the typically long distances between cell body and the injury site. Thus, promoting recovery of function after PNI and SCI by eliciting re-growth (regeneration) of the severed axons is a feasible repair strategy. One approach to axonal regeneration is to introduce exogenous axonal growth-promoting molecules to the site of injury. In this thesis, we have investigated the molecular mechanisms of action and the nervous tissue repair potential of polymers of acidic laminin (aLam), an injectable axonal growth-promoting biomaterial.

1.1   BIOMATERIALS

There is not yet a consensus among scientists and engineers on what constitutes a biomaterial, but here it is loosely defined as: "a naturally occurring or synthesized material exposed to a biological specimen separate from its origin to elicit a response." The emergence of biomaterials for regeneration and increased collaborations between engineers, basic and translational scientists, and clinicians hold promise for the development of effective therapies for spinal cord and peripheral nerve injury. A plethora of biomaterials are available and have been tested in various models of SCI (4) and PNI (5). Biomaterials may provide structural support and/or serve as a delivery vehicle for factors to arrest growth inhibition and promote axonal growth. Designing materials in order to address the specific repair needs of the damaged central nervous system is crucial and possible with current technology.

In general, biomaterials for nervous tissue repair are employed for their ability to provide passive structural or active growth support to damaged axons; some offer both through functionalization with biologically active peptide sequences. Numerous natural and artificial materials have been tested for their efficacy in repairing the injured central (6, 7) and peripheral nervous system (8, 9). Application of some of these resulted in functional improvements demonstrating their repair potential. As introduced above, axonal regeneration is considered an important repair mechanism for the injured nervous system and promoting regeneration of severed axons after injury could elicit anatomical and behavioral recovery.

Most biomaterials designed and produced in the laboratory and tested for their efficacy to repair the injured peripheral nerve and spinal cord are polymers. Polymers have numerous biomedical applications due to their vastly diverse properties. Typically, polymers are large 2-

or 3-dimensional molecules composed of repeating units (10, 11). Polymers can be obtained from natural sources including plants, animals, and deoxyribonucleic acid, or be fabricated synthetically in a laboratory. Natural polymers are widely available and tend to undergo highly controlled synthesis resulting in regular structures; however, they often contain contaminating molecules and are difficult to sterilize (11). Synthetic polymers are easier to sterilize, but are typically susceptible to the chosen process of synthesis often causing irregularities in structure and composition (11).

Currently, there is a lack in agreement in the literature on the optimal characteristics of biomaterials for promoting neural regeneration and repair. However, there is increasing theoretical and experimental evidence for the use of polymers for repair of soft tissue such as nervous tissue (6, 7). An important advantage of some polymers for nervous tissue repair is that they can be designed for *in situ* polymerization and/or cross-linking, therefore requiring less invasive approaches to be applied, i.e. injection. Other advantages are that they can be fabricated to degrade within a s pecific time window, they are non-cytotoxic, and they have similar mechanical properties as that of the host tissue to minimize fibrolysis (12).

A variety of natural biomaterials mostly present within the extracellular matrix (ECM) provide structural and growth support to axons in the developing (13, 14), mature (15), and damaged (16) nervous tissue. Laminin, collagen, fibronectin, vitronectin, and proteoglycans(PG)/glycosaminoglycans (GAGs) (14) are all members of this particular group of materials. Many axonal growth-promoting ECM components signal through integrin receptors (17) that often bind the Arg-Gly-Asp (RGD) peptide sequence (18). ECM proteins have been implemented as biomaterials to repair nervous tissue (19, 20) and increase compatibility of other materials interfacing with in the nervous system (21). Our continuously increasing

3

understanding of the role of ECM in axonal growth and regeneration has fueled many investigations of the repair efficacy of these particular materials (22).

1.1.1 Laminin

Laminin is a heterotrimeric glycoprotein consisting of alpha, beta, and gamma subunits that self-assemble in a temperature-, pH-, and concentration-dependent manner (2, 23). As a major component of basement membrane ECM, laminin has frequently been shown to influence neurite outgrowth both *in vitro* (2, 24-26) and *in vivo* (25, 27-30). There are fifteen different types of laminins that have been identified thus far. Plantman et al (12) showed that laminin-α1β1γ1 (laminin-1 or laminin-111) promotes neurite outgrowth of adult DRG neurons in culture in the absence of growth factors. Laminin is not a structurally robust ECM protein, and therefore quite suited for injection or as an adjunct in combination with other more supportive materials to increase cell growth (31-34) and differentiation (35).

One group has shown that the structure of the laminin-1 polymer may be a determinant in its signaling pathways and/or efficacy. Certain structural configurations may induce regeneration and functional recovery when injected directly into the spinal cord following injury(30).

1.1.2 Acidic Laminin Polymer

In vivo, laminin has been shown to assemble in different structures depending on environmental cues (23). Unlike some ECM molecules that require external factors for polymer formation, laminin is able to self-assemble, and readily does so in solution at room temperature (23).

Laminin-111 in particular has been shown to have the capability of assembling in different structural configurations in a pH-dependent manner (2). These different structural configurations will be referred to here as acidic laminin (aLam, identifying the polymer structure assembled in a pH4 environment) and neutral laminin (nLam, identifying the polymer structure assembled in a pH7 environment). Freire and colleagues showed that embryonic neurons grown on a substrate of aLam extend longer neurites than those grown on a substrate of nLam, without differences in number of adhered neurons or strength of cell attachment (2). These data suggest that the configuration of laminin can alter its neurite growth-promoting capability.

Laminin communicates with cells through binding to cell surface integrin receptors (36). The configuration of laminin could determine how it binds/activates integrins. Integrin activation regulates neurite outgrowth via formation and breakdown of focal adhesion complex and activation of Focal Adhesion Kinase (FAK) and mitogen-activated protein kinase kinase/extracellular signal-regulated kinase (MEK/ERK) signaling pathways leading to actin polymerization at the growth cone level and neurite extension (37).

1.2   INTEGRIN RECEPTORS AND THE FOCAL ADHESION COMPLEX

Integrin receptors are heterodimeric transmembrane proteins that consist of alpha and beta subunits, each with cytoplasmic tails that transmit information upon binding of a ligand to the cell. There are various integrins that mediate laminin-cell interactions (36). It has been shown that a crucial element for integrin dependent neurite growth is the $\beta1$ subunit (24, 38); $\alpha1\beta1$ and $\alpha3\beta1$ integrin receptors have specifically been implemented in laminin-111-mediated neurite growth *in vitro* (24, 26). The Arginine-Glycine-Aspartic acid (RGD) motif is present in laminin

and involved in integrin binding. Other motifs in laminin binding with different affinities to integrins result in a variety of cellular events (39). One of the cellular events cause by integrin signaling is the formation of the focal adhesion complex, which consists of a variety of proteins gathered together in a functional unit at the site of the cytoplasmic tails of the integrin receptors (Figure 1).
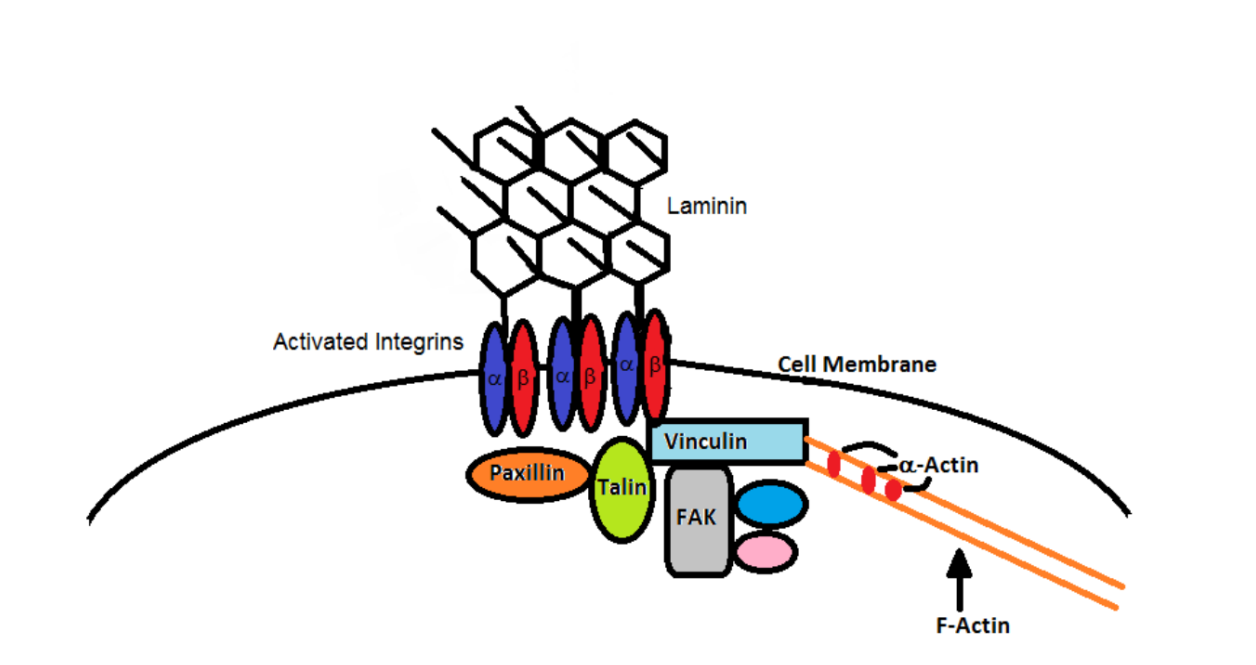
Figure 1. Schematic of Focal Adhesion Complex with some of the key proteins highlighted

One important protein within the focal adhesion complex is vinculin, which has been implemented in FAK autophosphorylation and actin polymerization specifically in the neuronal growth cone (40, 41). This occurs when integrin receptors are activated and cluster together on the cell membrane in response to binding a ligand (42). The ligand-receptor interaction can be

described as a dynamic equilibrium process where R is the receptor and L is the ligand and C is the receptor-ligand complex (Equation 1)(42).

Equation 1

$$R + L \leftrightarrow C$$
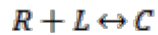
Once receptors are activated and clustered and the focal adhesion complex is formed, there is a change in the association constant (*Ka*) of the ligand-receptor interaction (Equation 2) (16). The clustering of the receptors to form this complex results in a change in the probability of the ligand being bound to the receptor, thereby increasing the concentration of receptor-ligand complexes.

Equation 2

$$[C] = K_{\alpha}'[R_0][L_0]$$

Due to its natural role in promoting and guiding growth of axons in the developing CNS and adult PNS and the lack of effective axonal growth-promoting strategies when damage occurs, the potential of laminin to elicit axonal regeneration after nervous tissue injury is of clinically relevant interest. Since aLam was found to be a better promoter of neurite extension than nLam, which is the typically used laminin polymer substrate in neuronal cultures, investigation of the mechanisms underlying aLam-induced axonal growth is of particular importance as it may reveal novel therapeutic targets that would support the development of materials that effectively promote axonal regeneration after nervous tissue damage. Having a well-characterized *in vitro* model system for screening/evaluating materials for growth dynamics under live imaging would be a highly valuable tool.

7

1.3   MICROCONTACT PRINTING FOR LIVE IMAGING ASSESSMENT

Microcontact printing (μCP) is a combination of soft lithography and stamp printing, most often performed with polydimethylsiloxane (PDMS) stamps made from etched glass or silicon master reliefs. This technique was first utilized to pattern gold (43) and has since been utilized in many electronic and cellular biology applications. One important benefit of using this technique is that the etched glass or silicon master relief allows for a high degree of pattern reproducibility. A stamp can be used many times and easily be replicated in case some damage occurs. The concept behind μCP is that a particular material is used to create a reservoir of "ink" absorbed into the PDMS stamp (Figure 2). This technique allows for μm level control over patterning of a substrate and, therefore, in biological applications, μm level control over the direction and surface to which cells will attach and migrate and/or grow.
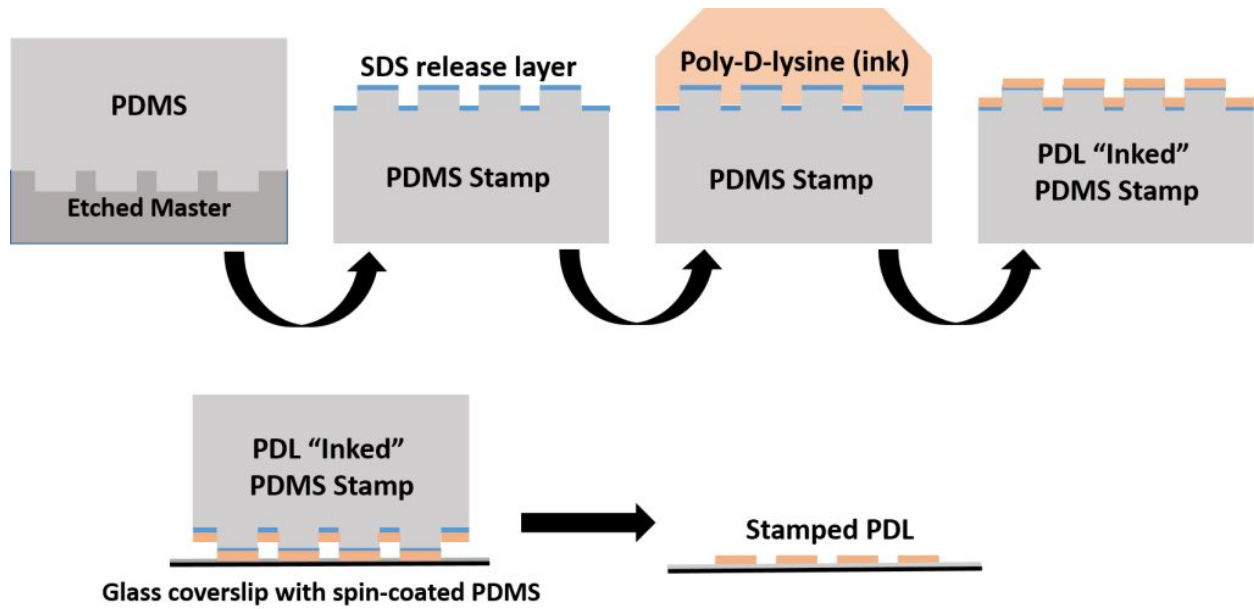
Figure 2 Microcontact Printing with 10% w/v SDS release layer

Previously, using printing of a variety of ECM and non-ECM substrates, this technique has been shown to direct both neuronal and non-neuronal cell attachment and growth (44-48). An additional advantage is that this technique allows tracking of axonal growth cones because of the pattern-directed growth. On a non-patterned substrate axons will grow indiscriminately in all directions, making accurate quantifiable comparisons of dynamic growth difficult. The pattern-directed growth of axons on stamped substrates, however, allows for easier tracking and thus measuring of growth speed and cell-cell interactions.

1.4 PERIPHERAL INJURY AND REPAIR

In the US, up to 5% of people entering level 1 trauma centers have some type of damage to the peripheral nervous system leading to paralysis and/or neuropathic pain (5). The axons injured in PNI derive from motor neurons located in the spinal cord ventral horn and/or sensory neurons located in the dorsal root ganglia. Because PNI occurs frequently on the battlefield much of our current knowledge has been gathered in wars such as the American Civil War and the World Wars I and II (49-51). Due to the high variety of causes and the fact that injured nerves may contain either motor or sensory axons or both, the level of ultimate impairment (and recovery) is often unpredictable. PNIs are most commonly categorized using the Seddon (49) or Sunderland (50) classification scheme. Seddon classifies injuries into three categories termed "neurapraxia" (intact axon, loss of myelin or ischemia), "axonotmesis" (axon loss and variable stromal disruption) and "neurotmesis" (axon loss and complete disruption of endoneurial tubes, perineurium and epineurium) (49). Sunderland classifies injuries in five degrees, the first of which is equivalent to Seddon's "neurapraxia" and the fifth to "neurotmesis". In Sunderland's classification scheme, the "axonotmesis" classification is further divided into second, third and fourth degree injuries depending on the degree to which the endoneurial tubes, perineurium and epineurium are intact or disrupted(50).

While axons in the damaged peripheral nerve exhibit a relatively high intrinsic level of regeneration, the recovery of function is typically limited and largely dependent on the size and location of the defect. Injuries causing greater than second degree severity typically require some surgical intervention (52). Currently, the gold standard in surgical repair of moderate to long distance PNI is grafting of an autologous nerve, commonly the sural nerve, which connects proximal and distal nerve stumps and provides a Schwann cell-filled guidance conduit for

growth-promotion and guidance of severed axons (53). This gold standard approach remains suboptimal in that it invariably leads to loss of function at the donor site, and potential mismatch in graft size. An alternative approach is the use of allogeneic genic grafts but these require immune suppressors which may cause unwanted side effects. Time is of the essence when considering surgical treatments for PNIs. If a motor nerve is damaged, the treatment window for axon regeneration and re-innervation is 18-24 months, after which time muscle atrophy is often an unsurmountable obstacle to functional recovery (52). This therapeutic window is longer if the lesion is to a sensory nerve since their target end organs generally degrade much slower (52). To maximize the overall level of functional recovery after PNI, treatments designed to encourage and/or enhance axonal regeneration should be implemented as soon as medically possible, especially with injuries involving motor axons.

The use of biomaterials for peripheral nerve repair has received ample attention in the last decade. It is a rapidly expanding field of pre-clinical and clinical research. Due to the relative accessibility of many peripheral nerves, many strategies involving conduits have been investigated for their PNI repair potential. Conduits become especially important in neurotmesis injuries where the guidance provided by the perineurium and epineurium has been disrupted. When one or more of these sheaths are left intact, as in axonotmesis injuries, injectable, growth-promoting molecules/materials may be preferred as they do not carry the risk of nerve compression associated with conduits.

1.5   SPINAL CORD INJURY AND REPAIR

SCI produces an immediate and ongoing loss of nervous tissue often resulting in (thus far) untreatable loss of function, which has devastating personal and societal consequences. The most prevalent mechanism of SCI in humans is a contusion which typically presents in the formation of fluid-filled cystic cavities in the central spinal cord surrounded by a rim of spared white matter. These anatomical incomplete contusions often result in complete loss of motor and sensory function. A recent study conducted by the Dana and Christopher Reeves Foundation revealed that approximately 1.27 million people in the US alone are living with some type of paralysis as a result from SCI (54). In the US, each year, there are approximately 12,000 new cases of SCI, which means that the group of people living with a spinal cord injury is steadily growing (54). SCI results in physiological, sociological and psychological problems and a range of functional impairments, which are mostly dependent on the type, severity, and location of the initial injury. Medical expenses and lifestyle changes associated with these injuries are costly to both the injured individuals and society. Depending on the level and severity of injury, the lifetime cost of SCI ranges between 0.5-3 million dollars per patient (54). The personal and societal consequences of SCI drive the search for treatments that lead to biologically significant recovery of function (54, 55).

There are three main mechanisms that are thought to contribute to recovery of function after a SCI: neuroprotection, rehabilitation, and regeneration. Neuroprotective approaches aim to limit the secondary loss of healthy nervous tissue which may lead to decreased overall loss of function and/or increased prospects for future repair strategies. Neuroprotective approaches need to be initiated soon after injury to maximize the reparative effects. Rehabilitation, typically through physical therapy and/or electrical stimulation paradigms, aims to induce axonal plasticity

in spared axonal circuits that could lead to reorganization and increased functional connectivity. Regenerative approaches aim to promote axonal re-growth and re-connection with the original or new target neurons which could alone or in combination with targeted rehabilitative strategies lead to increased recovery of function. The studies described in this thesis focus on an approach to promote axonal regeneration. Axonal severance after SCI leads to interruption of signaling between the brain and spinal cord segments below the injury site and, ultimately, the periphery. Adult mammalian neurons retain the intrinsic ability, albeit to a limited degree, to regenerate their damaged axon. However, the lack of (nervous) tissue, which could serve as a growth substrate, and the presence of axonal growth-inhibitory molecules, expressed by reactive astrocytes and in oligodendrocyte myelin debris, in and around the injury site, limit regeneration of axons and, consequently, their contribution to functional recovery. Previous studies have shown that the introduction of axonal growth-promoting molecules/materials in the injured spinal cord may elicit axonal regeneration which in some, but not all, cases was accompanied by functional improvements. These partially successful studies are a major motivation for the development of novel more effective axonal regeneration-promoting biomaterials.

1.6   GOALS OF THESIS

The goals listed below guided the planning and design of each of the studies included in this Thesis. The chapters in which the studies are described is listed in parenthesis. All study results and future directions are discussed in the General Discussion section (Chapter 4).

1) To develop and utilize a novel *in vitro* system to test the molecular and cellular mechanisms of aLam as a growth-promoting molecule (Chapter 2.1)

2) To employ microcontact printing and live imaging to create a system in which to study aLam's effect on growth cone dynamics and glial cell involvement (Chapter 2.2)

3) To test the repair potential of aLam as an injectable regenerative therapeutic using an adult rodent model of PNI (Chapter 3.1)

4) To test the repair potential of aLam as an injectable regenerative therapeutic using an adult rodent model of SCI (Chapter 3.2)

2.0 SIGNALING MECHANISMS OF ACIDIC LAMININ-MEDIATED AXON GROWTH IN VITRO

Previous studies showing that a substrate of aLam enhances neurite growth of embryonic cortical neurons *in vitro* (2), supporting the development of aLam as a therapeutic for nervous tissue repair. At present, the mechanisms underlying the axon growth-promoting ability of aLam are unknown. Elucidating these mechanisms will expand our current knowledge and possibly reveal novel targets supporting the development of more effective strategies to promote axonal regeneration and functional recovery after nervous tissue damage.

2.0.1 *In vitro* model system

The *in vitro* model systems typically used to investigate the potential of particular molecules to elicit and/or enhance neurite outgrowth contain embryonic neurons growing on a substrate of the molecule in question. The main reason is that embryonic neurons, in contrast with adult neurons, retain their growth competence to a relatively large degree, allowing for a less demanding evaluation of the neurite outgrowth. Previously, the effects of aLam on neurite outgrowth has been studied using embryonic neurons cultured on a substrate of aLam(1). However, the vast majority of injuries to peripheral nerves and the spinal cord occur in the adult and are 'closed injuries' with an intact epineurium and dura mater, respectively, which would be

best treated using injectable therapeutics. So far, the effects of injectable, non-substrate, aLam on neurite outgrowth of adult neurons are unknown. We have developed here a novel *in vitro* model system containing adult neurons with aLam presented as an unbound therapeutic to better model the specific circumstances of the majority of PNIs and SCIs (Figure 3). In this novel culture model system, the neurons are grown on poly-d-lysine (PDL) which itself provides no support to neurite outgrowth. We have used this model system to evaluate the effects of aLam on neurite outgrowth on the molecular level, using antibody blocking and SDS-PAGE and Western Blot, and the cellular level, using live cell imaging and immunocytochemistry (Chapter 2.1). In order to elucidate what occurs during an active growth period, a microcontact printed pattern of PDL was tested in its ability to guide neuronal outgrowth and allow for a more rigorous and clear visualization of the dynamic growth process (Chapter 2.2).
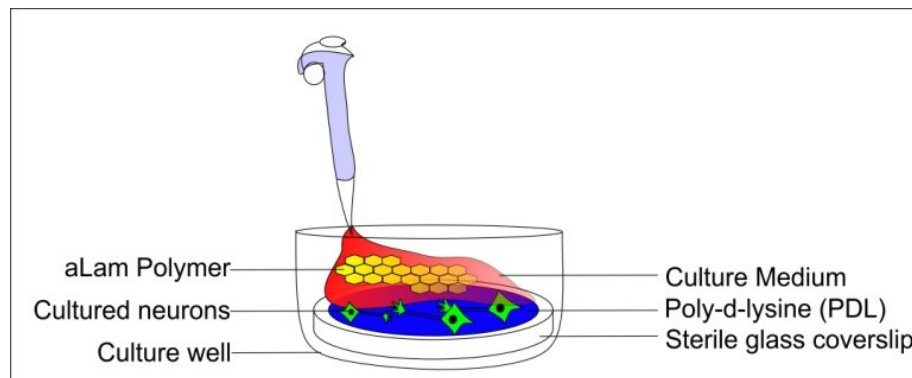
Figure 3 *In vitro* model system

With this model we enabled investigation of the effects of different laminin structures (aLam and nLam) on integrin binding and activation and neurite growth. This provided novel

insight into the testing of signaling capability of self-assembling ECM molecules in an environment where they are not acting as a primary substrate for cell attachment. This system can potentially be used to differentiate between factor-like signaling and substrate-signaling of a variety of ECM molecules/binding motifs that have so far only been investigated as a substrate for neurons. T his is a new and innovative *in vitro* approach to studying 'substrate-like' molecules that are being investigated as injectable treatments following spinal cord and peripheral nerve injury.

2.1   ACIDIC LAMININ POLYMER AND INTEGRIN-MEDIATED SIGNALING

2.1.1   Introduction

Regeneration of axons (or lack thereof) following a traumatic injury to the nervous system is a widely studied, yet somewhat poorly understood phenomenon. T here are both intrinsic and extrinsic factors that contribute to the anatomical and physiological outcome. Studies of intrinsic factors are mostly focused on t he intracellular changes occurring naturally with age, or as a consequence of damage, including gene expression, protein transport and physiological properties. E xtrinsic factors contributing to the level of endogenous axon regeneration in damaged nervous tissue include invasion and activation of inhibitory macrophages and microglia, scar formation, myelinating glial state changes, availability of growth factors and the breakdown in both structure and function of the extracellular matrix (ECM). ECM provides important scaffolding for cellular growth as well as a signaling ligand for membrane-bound receptors. T hese cell adhesion receptors affect gene expression for growth, direction and

apoptotic signaling cascades within the cells. Different components of the ECM typically define the niche in which a cell resides. Much of CNS development is driven and arrested through ECM (and other non-matix extracellular signaling molecules)-receptor interactions. The integrin family of receptors, specifically, interact with many of the different ECM proteins including fibronectin, collagen and laminin (56). In order to evaluate the mechanisms of structurally different laminin polymers for axon outgrowth, the *in vitro* experiments described here have been purposefully designed to gather information about its potential for use as a signaling molecule interacting with adult, terminally differentiated neurons. We will test the **hypothesis** that *aLam signals through integrin receptors in order to promote the neurite outgrowth competence of adult neurons in vitro.*

2.1.2 Materials and Methods

2.1.2.1 Reagents

aLam and nLam: Laminin-111 (Invitrogen, 1mg/ml in saline) was diluted to a final concentration of 50μg/ml in either a Tris buffer (20mM, pH 7, nLam) or Sodium Acetate buffer (20mM, pH 4, aLam) as described in (2). ALam or nLam was suspended in culture medium for cellular exposure.

Dissociation and Culture Media: Dulbecco's Modified Essential Medium (DMEM) + 10% Fetal Bovine Serum (FBS) + 1% Penicillin Streptomycin (Pen/Strep).

2.1.2.2 Neuron cultures

DRG dissection and culture protocol were modified from Malin et al (57) for use with adult rat neurons cultured on poly-D-lysine. Dorsal root ganglia (DRG) neurons were harvested from the

L3-L5 spinal section of adult female Sprague-Dawley rats (200-250 g) under deep sedation of Ketamine (90 mg/kg)/ Dexmedetomidine (0.75 mg/kg) (IP) to maintain the integrity of the neurons. Laminectomy was performed to expose L1-L6 spinal cord and the L3-L5 DRG pairs (6 ganglia total) were dissected (Figure 4). Individual ganglia were thoroughly cleaned from blood and nerve fragments and dissociated enzymatically (10 min papain (40 units/mL, Worthington, #3126) followed by 20 min collagenase type II (1580 units/mL, Worthington, #4176)/dispase type II (8.5 units/mL, MB, #165859) under agitation at 37 ºC) and mechanically (15 x trituration in HBSS (-Ca -Mg) with fire-polished glass pipette, centrifuge at 4.5 min, 3000 g to pellet 2x). The cells were transferred to pre-warmed culture medium (37ºC) and 100 uL of cell suspension was added to each poly-d-lysine (PDL, 100 µg/mL, Millipore, #A-003-E) coated 15 mm glass cover slip (Ted Pella, #26021) in a 12-well plate and placed into a humidity controlled incubator (5 % CO_2/37 °C). After 2 h, neuronal cultures were treated with either culture medium alone or culture medium containing 10 % aLam or nLam (50µg/mL), followed by 24 h incubation. Cultures were then prepared for either immunostaining or gel electrophoresis.
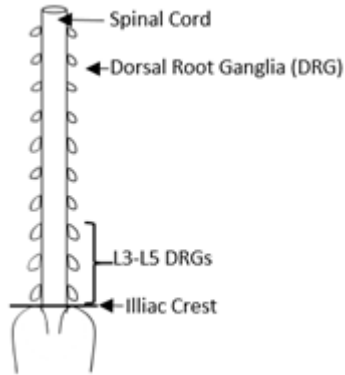
Figure 4 Schematic of rat spinal cord with dorsal root ganglia (DRGs). Location of L3-L5 ganglia lies directly rostral to iliac crest

2.1.2.3 Immunostaining and Axon Length Quantification

Cell cultures were fixed with 4 % paraformaldehyde (PFA) for 10 m in at room temperature. Nonspecific binding sites on fixed cells were blocked using 5% Normal Goat Serum (NGS) and permeablized with 0.3 % Triton in .01M Phosphate Buffered Saline (PBS) for 30 m inutes at room temperature. C ells were then incubated with primary antibodies diluted in blocking solution for either 2 h a t room temperature or up to overnight at 4 °C (Table 1). Fluorescent secondary antibodies diluted in 0.01 M PBS (Alexa Fluor®, life technologies) (Table 1) were added for 1 h a t room temperature, followed by DAPI counterstaining and coverslips were inverted onto microscope slides. Axon lengths were determined using a Zeiss Axio Observer inverted fluorescent microscope with Zeiss Plan Apochromat objective (20 x air, NA 0.8), and Neurolucida (MBF Bioscience) software. Slides were relabeled to blind experimental conditions and the 10 ne urons with the most substantial growth from each coverslip (minimum 3 coverslips/condition) were identified for tracing and quantification. Each experiment contained

3 biological replicates and at least 3 technical replicates. Graphs are pooled results of all cells analyzed (minimum 90 cells/group).

2.1.2.4 Integrin Blocking

Cells were harvested and plated as described above. Following plating, cells were incubated at 37 °C and 5 % CO_2 with integrin-blocking antibodies at a concentration of 20 µg/mL (see Table 1) in culture medium for 2 h. Then, fresh culture medium alone or containing aLam or nLam was added to each well, and the incubation continued for 24 h. The cells were then prepared for either immunocytochemistry or protein gel electrophoresis. PDL was chosen as a cell substrate for all *in vitro* experiments because it binds neurons non-specifically, so that initial cell adhesion did not confound the evaluation of integrin-laminin interactions.

2.1.2.5 Electrophoresis and Western Blot

In order to obtain enough protein for detection, cells from six pairs of DRGs (L1-L6)/2 rats were dissected and cultured for 24 h as described above. The cells were then trypsinized using manual agitation for 12 min, rinsed, and lysed using PMSF-RIPA buffer. The proteins from the cell lyses were combined with Laemmli Buffer (3:1) in boiling water for 5 min, placed on wet ice and separated by denaturing polyacrylamide gel electrophoresis (SDS-PAGE) (125 V, 75 min) using Novex® precast Tris-glycine gels (life technologies, EC60255BX5). A total of 15 µL lysate+buffer was loaded per well and transferred overnight at 4 °C to nitrocellulose membranes (100 V).

2.1.2.6 Protein Staining and Visualization

Nonspecific binding sites of proteins on the membranes were blocked using 1 x TBS-T + 5 % blocking (Bio Rad, #107-6404XTU) 1 h at room temperature. Membranes were then incubated with primary antibodies diluted in blocking solution (see Table 1) for 1 h at room temperature followed by overnight at 4 ˚C. After rinsing, membranes were exposed to Horseradish Peroxidase (HRP)-conjugated secondary antibodies for 1 h at room temperature. Protein bands were visualized using enhanced chemiluminescent (ECL) substrate (SuperSignal West Femto, ThermoScientific, #34095) followed by 10 s ec exposure to ECL Hyperfilm and developed. Quantification was performed using ImageJ software gel analysis tool (58).

Table 1 Working Concentrations of Primary and Secondary Antibodies

Experimental Procedure	Antibody Specifications	Working Concentration (μg/mL)
Immunocytochemistry	Anti-ß-III Tubulin (purified rabbit monoclonal; Covance, MRB435P)	0.5
Immunocytochemistry	Alexa Fluor 488 (α-rabbit, IgG; Molecular Probes, A11008)	0.4
Antibody blocking	Anti-α1 Integrin (rabbit polyclonal; Antibodies-online, ABIN343462)	20
Antibody blocking	Anti-α3 Integrin (mouse monoclonal; BD, 611044)	20
Antibody blocking	Anti- α5 Integrin (rat monoclonal; antibodies-online, ABIN135245)	20
Antibody blocking	Anti- α6 Integrin (CD49f, purified rat monoclonal; BD, 555734)	20
Western Blot	Anti-GADPH (rabbit polyclonal; Sigma, G9545)	0.125
Western Blot	Anti-ß-III Tubulin (purified rabbit monoclonal; Covance, MRB435P)	1
Western Blot	Vinculin (mouse monoclonal; Sigma, V9264)	0.1
Western Blot	Anti-α3 integrin (mouse monoclonal; BD, 611044)	0.5
Western Blot	Anti-α1 Integrin (rabbit polyclonal; Antibodies-online, ABIN343462)	1
Western Blot	Goat α-rabbit (IgG, HRP; Invitrogen, G21234)	0.2
Western Blot	Goat α-mouse (IgG, HRP; Invitrogen, G21040)	0.2

2.1.2.7 Statistical Analysis

Differences in outgrowth data was tested using the Kruskal-Wallace test for nonparametric data in SPSS software package (SPSS version 21, IBM). Data, as expected failed homogeneity of variance assumption required for standard ANOVA testing (medium only group had very low variance as most cells grew very little or not at all, while other groups had some cells with very limited and others that had extensive outgrowth). All other measurements satisfied assumptions and therefore F-statistic (ANOVA) was calculated using SPSS statistical software package. Significance was set at ≤ 0.05.

2.1.3 Results

2.1.3.1 aLam promotes neurite growth from adult DRG neurons *in vitro* better than nLam

No difference in neuronal attachment was detected between groups ($p > 0.05$, data not shown) with all cells plated on PDL coated glass coverslips. Photomicrographs are presented in Figure 5 to illustrate the outgrowth of the neurons under the various conditions. Q uantification demonstrated that neurons presented with aLam exhibited significantly greater neurite outgrowth ($p < 0.001$) than those presented with nLam or medium only (Figure 5).
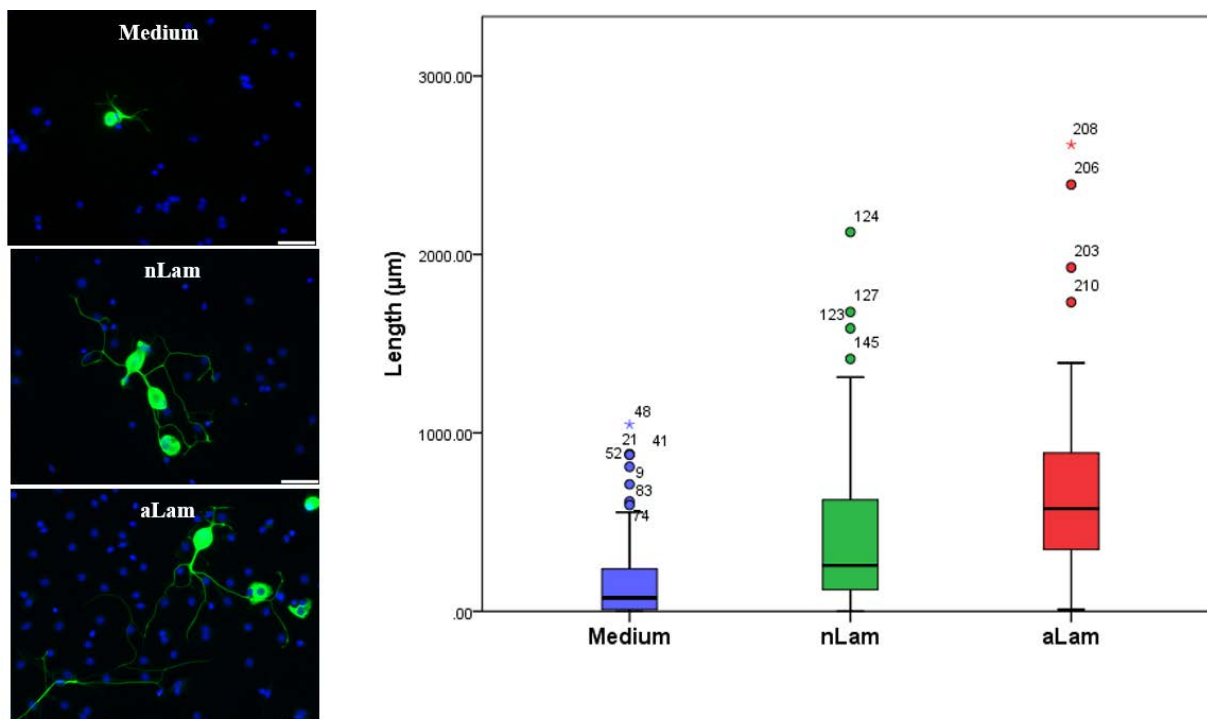
Figure 5 Neuronal Outgrowth Profiles. *Graph:* Box Plot of median neurite outgrowth per group after 24hr incubation, Independent-Samples Kruskal Wallis test significance <.001 between groups. *Images:* Acidic laminin (aLam), Neutral laminin (nLam), Medium alone (βtubulin-III (green), DAPI (blue); scale bar = 50μm. Note: Brightness of all color channels equally enhanced to better visualize outgrowth).

2.1.3.2 aLam and nLam exhibit differential interactions with α1 and α3 integrins

We used integrin blocking to study laminin-cell communication. Immunocytochemistry for α1 and α3 integrins revealed that both receptors are present on the neurons in our cultures prior to exposure to laminin (Figure 6). With any of the used antibody combination, differences in cell adhesion of the neurons were not observed (p > 0.2, data not shown).

24

With blocking of α1 integrin only, the growth-promoting capabilities of aLam, but not nLam were unaffected. T he average measured outgrowth of cells exposed to aLam was unchanged following α1 integrin blocking relative to unblocked aLam control ($p > 0.3$), while that of cells exposed to nLam was significantly decreased ($p < 0.01$) (Figure 6).

With blocking of α3 integrin only, the neurite growth responses did not significantly decrease in aLam or nLam groups relative to unblocked controls ($p > 0.05$). On the other hand, blocking of both α1 and α3 integrin resulted in a significant decrease in outgrowth of neurons in aLam ($p < 0.001$) and nLam ($p < 0.01$) (Figure 6).
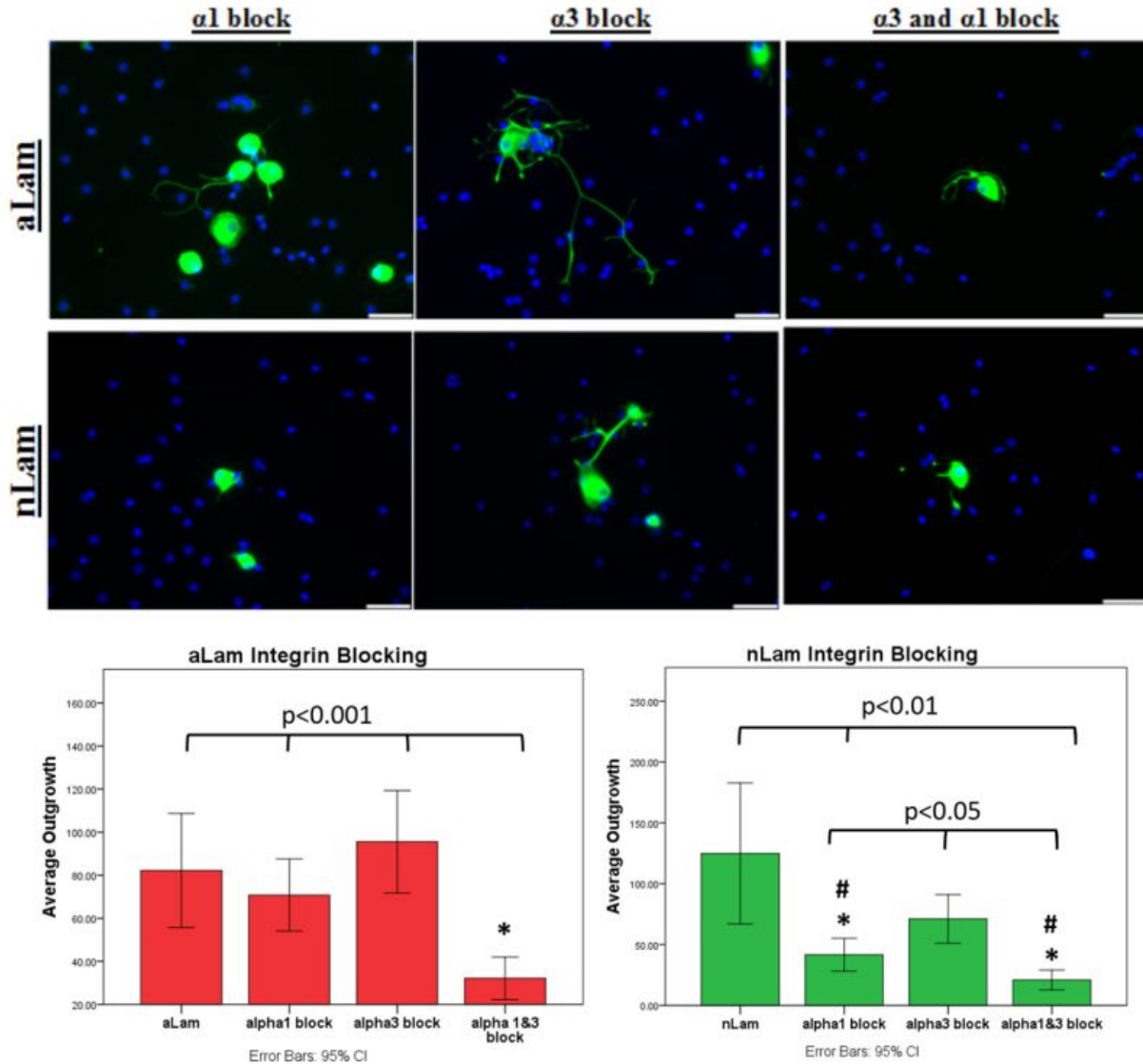
Figure 6 Neuronal Outgrowth Profiles after Antibody Blocking. *Images:* DRG neurons plated on poly-D-lysine with antibody blocking of α1 integrin(first row), α3 integrin (second row) and α1+ α3 integrins (third row), +aLam added to culture (first column), +nLam added to culture (second column). (βtubulin-III (green), DAPI (blue); scale bar = 50μm); Note: brightness of all color channels equally enhanced to better visualize outgrowth in images. *Graphs:* Mean neurite outgrowth (μm) per each condition. For aLam condition * denotes $p < 0.001$; for nLam condition * denotes $p < 0.01$, # denotes $p < 0.05$.

To test the specificity of the α1 and α3 integrin involvement in laminin-mediated neurite outgrowth, additional controls for the blocking experiments that included α5 (a non-laminin associated integrin) and α6 (a non-growth laminin-associated integrin) were similarly evaluated with immunostaining/axon quantification analysis. The results showed that neither α6 nor α5 blocking resulted in significant decrease in outgrowth (p >0.05) under either experimental condition (data not shown), suggesting that aLam and nLam signal their neurite growth activity through α1 and α3 integrins.

2.1.3.3 Blocking α1 integrin leads to laminin structure-dependent changes in the relative expression of α3 integrin

Protein electrophoresis and western blotting were performed on cell lysates from integrin blocking experiments to calculate the relative protein concentrations. We confirmed that the levels of glyceraldehyde 3-phosphate dehydrogenase (GADPH) were similar between groups, allowing it to be used as a standard to compare integrin levels (Figure 7). In the unblocked condition, there are similar relative expression levels of α1 and α3 integrins in the presence of either aLam or nLam (Figure 7A, C). When α1 integrin was blocked, followed by exposure to aLam, cells exhibit a relative increase in the expression of α3 integrins (Figure 7, D). When α1 integrin was blocked, followed by exposure to nLam, no change in α3 integrin expression was detected (Figure 7, B).
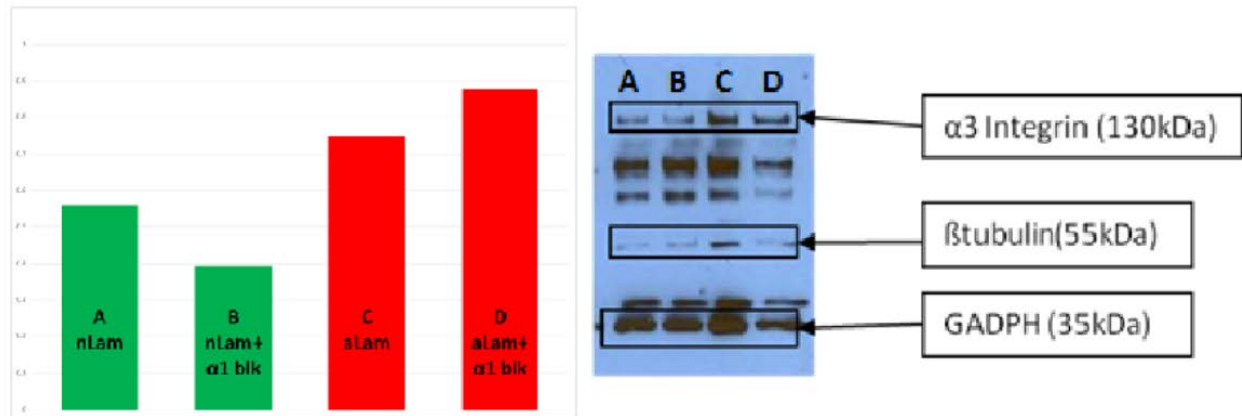
Figure 7 Increased α3 Integrins Expression After α1 Block. A) Relative α3 integrin protein levels from unblocked DRG cell lysates exposed to nLam. B) Relative α3 integrin protein levels from cell lysates where α1 integrin has been blocked followed by exposure to nLam. C) Relative α3 integrin protein levels from unblocked DRG cell lysates exposed to aLam. D) Relative α3 integrin protein levels from cell lysates where α1 integrin has been blocked followed by exposure to aLam.

2.1.3.4 The presence of aLam increased relative amounts of Vinculin

Total amounts of vinculin in cultures containing aLam, nLam or media alone were evaluated using SDS-PAGE and Western Blot. These semi-quantitative results revealed relative increases in vinculin protein concentration compared to GADPH levels. The highest level of vinculin was found in neurons exposed to aLam, while the lowest levels were found in neurons exposed to medium only (Figure 8).
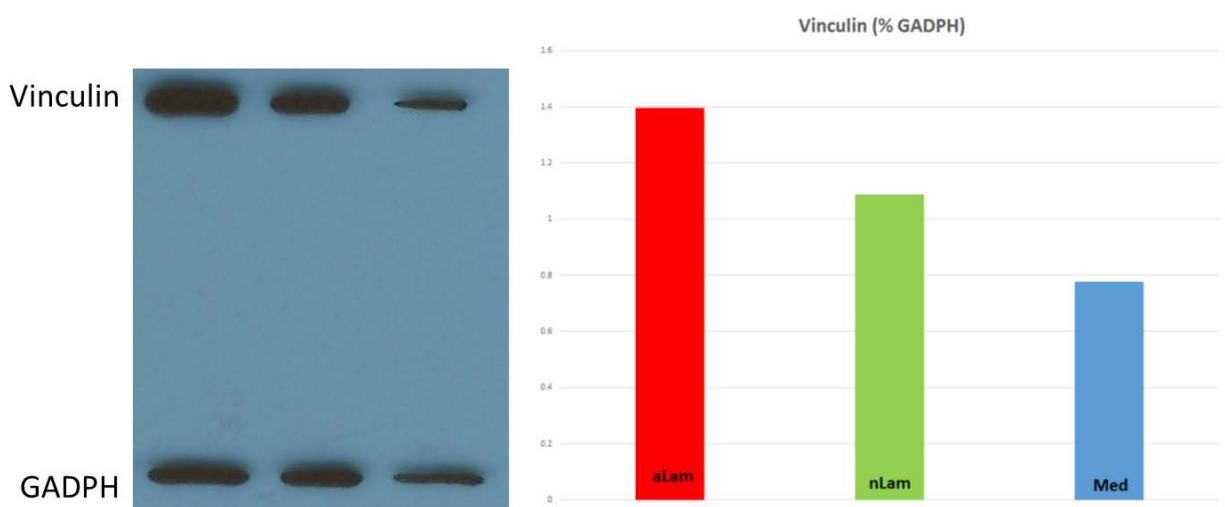
Figure 8 Vinculin Protein Expression Levels. Relative vinculin protein levels in cell lysates from DRG cultures exposed to aLam are greater than nLam or medium alone.

2.1.4 Discussion

Laminin is known for its effects on neural outgrowth *in vivo* during development and as a substrate for attachment in neuronal cultures *in vitro*. So far, the effects of laminin as an unbound signaling molecule for neurite outgrowth *in vitro* have not been investigated. In the present *in vitro* study we demonstrate that: 1) aLam and nLam can act as a signaling molecule to promote neurite outgrowth of adult neurons; 2) aLam is a significantly stronger promoter of outgrowth of adult neurons *in vitro* than nLam; 3) aLam and nLam convey their actions differentially through α1 and α3 integrins; 4) aLam, but not nLam, causes upregulation of α3 integrins under blocking of α1 integrin; 5) aLam causes an upregulation of vinculin. Our findings support the notion that unbound aLam promotes enhanced outgrowth *in vitro* by increasing integrin activation leading to enhanced actin polymerization and neurite growth. The

29

data from this study confirm the use of aLam as a signaling molecule to promote neurite outgrowth *in vitro* and its potential to affect axon regeneration in damaged nervous tissue.

We demonstrate that laminin polymers can act as a signaling molecule to promote neurite outgrowth of adult neurons *in vitro*, and that aLam, is a superior to nLam in growth promotion signaling. To our knowledge this is the first demonstration that laminin polymers act as a signaling molecule enhancing the neurite outgrowth competence of adult neurons. The finding that aLam is a stronger promoter of neurite outgrowth than nLam agrees with earlier observations made in an *in vitro* model system containing embryonic neurons on a substrate of the two laminin polymers (2). However, our novel model system introduces two important features which significantly enhance the clinically relevance of the potential use of laminin polymers as nervous tissue repair-supporting molecules. One, we employed adult neurons which is an important and clinically relevant expansion of our current knowledge that aLam enhances neurite outgrowth of embryonic neurons (2), because the majority of nervous tissue injuries occur in adults. Two, we presented unbound, free, laminin polymers to the cultured adult neurons, rather than as a bound substrate, which is clinically relevant because most injuries to peripheral nerves and spinal cord are 'closed injuries' that prefer the use of injectable therapeutics. Together, the demonstrated enhancement of the neurite growth-promoting competence of cultured adult neurons of injectable laminin polymers open new avenues for using the development of effective strategies for repair of damaged nervous tissue.

We used molecular biology techniques to start understanding how aLam supports the neurite outgrowth abilities of neurons. Previous studies have suggested that laminin-111 signals

its growth promoting effects though α1 and α3 integrins, although there are a variety of integrin receptors for laminin. Our results revealed that both aLam and nLam signal their neurite growth-promoting actions also through the α1 and α3 integrins. The use of these two receptors appears to be specific for these polymers because we also showed that α5 integrins, which do not bind laminin, and α6 integrins, which bind laminin but is not primarily involved in neurite outgrowth, were not involved in aLam and nLam-mediated actions on neurite outgrowth in our model system.

If both types of laminin polymers signal through the same two receptors, how can then their total effect on neurite outgrowth be different? One possible reason is that the different polymers have different effects on the presence of the integrins on the cell surface. In general, an increase in the total amount of integrins would cause a stronger output. Our data did not support the idea that aLam would elicit an increase in the total amount of either α1 or α3 integrin. Interestingly, our integrin blocking experiment demonstrated that aLam, but not nLam, causes a relative increase in α3 integrin when α1 integrin was blocked. The role of this up regulation of α3 integrin by aLam, under non-physiological circumstances, is unknown but may indicate a compensatory effect to preserve the overall outgrowth effect. This may be of importance for future applications under conditions where neurons do not express or only express the α1 integrin to a low degree. This finding enhances the overall impact of aLam as a neurite growth-promoting molecule. Future studies aiming at evaluating neural selectivity of the growth-promotion elicited by aLam are needed to further elucidate this phenomenon.

An alternative, or complementary, reason for our observed differential effects of the polymers on neurite outgrowth even though they bind the same integrin receptors, is differential levels of activation. Upon ligand binding to integrins, intracellular events initiate clustering of

various proteins forming a focal adhesion complex. One of the crucial protein components of this complex is vinculin and our data demonstrate that the expression of this protein was increased in the presence of aLam. These findings indicate that aLam causes an increase in integrin activation which could lead to enhanced actin polymerization and neurite outgrowth.

The knowledge of multi-integrin binding of the polymers resulting in enhanced neurite growth is important for the future development of synthetic biomaterials to be employed in nervous tissue repair strategies. Based on this, such biomaterials could be designed to mimic aLam in its potential to elicit growth by enhanced formation of the focal adhesion complexes via co-binding α1 and α3 integrins. Another way to interpret this finding is to consider the potential of laminin in this configuration to have a complementary binding site, as is the case in fibronectin (59). Possibly, such a structural configuration could bring two integrin-binding ligands into close proximity, allowing for different binding affinity or activation state. If this is the case, the specific structure and presentation of binding ligands relative to one another is essential to elicit outcomes. Future studies testing this hypothesis by presenting these two peptides in close proximity at an optimal distance may further improve effects on neurite outgrowth.

2.2   MICROCONTACT PRINTING OF POLY-D-LYSINE FOR LIVE IMAGING

ANALYSIS OF AXON GROWTH

2.2.1   Introduction

Microcontact printing (µCP), a method for patterning substrates on a micron level accuracy, is a useful tool for creating patterns for directed growth on specialized culture dishes or coverslips specifically designed for use with live imaging. This technique is especially enticing because it can utilize many different substrates, including growth inert ones, like poly-d-lysine, for the targeted evaluation of growth-promoting molecules delivered in the media. This gives it an advantage over other growth-directing tools such as microfluidic devices, which require a minimal amount of growth-promotion within the substrate in order for axons to enter the designated chambers. When we attempted to use microfluidics for evaluation of unbound laminin with a PDL substrate, all growth remained within the soma reservoir and little to none was not drawn into the axon chambers, this phenomenon did not occur when laminin was used as a substrate. For our purposes here, developing this system into a successful tool for use with PDL and live imaging of neurite growth could provide valuable information not otherwise readily available.

In this study, we utilize the µCP technology to guide neurite outgrowth of adult neurons in order to track and quantify additional aspects of growth mediated by laminin polymers using live imaging and differential interference contrast (DIC) microscopy.

In this chapter we will test the **hypothesis** *that utilizing µCP patterned PDL substrates will allow for neuronal tracking to evaluate aLam elicited growth dynamics, including secondary interactions with glial cells and an increase in growth speed.*

2.2.2 Materials and Methods

2.2.2.1 Reagents

Culture Medium: The culture medium contained 25 mL Neurobasal®-A (Gibco) + 0.5 mL B-27 + 0.5 mM Glutamine + 1 % Penicillin Streptomycin (Pen/Strep).

Imaging Medium: The medium used for imaging contained the culture medium + 25 mM HEPES.

aLam and nLam: Laminin-111 (Invitrogen, 1 mg/ml in saline) was diluted to a final concentration of 50 µg/ml in either a Tris buffer (20 mM, pH 7, nLam) or Sodium Acetate buffer (20 mM, pH 4, aLam) as previously described (2) and as used on our *in vitro* investigation of the underlying mechanisms (see Chapter 2.1). ALam or nLam were suspended in culture medium before added to neuronal cultures.

2.2.2.2 Preparing culture dishes

Using a bench top drill press equipped with a ½ inch hollow bit, 35 mm culture dish was fixed onto a stage and a hole drilled in the center of the dish. Edges were smoothed to ensure a clean, flat surface for attachment of a 25 mm PDMS spin-coated glass coverslips. The coverslips were attached using a thin layer of PDMS along the edge of the drill hole on the inside of the dish and gently pressing it to ensure a seal is made. Dishes are then cured for 24 h at 65 ºC. To sterilize, dishes with attached coverslips are treated in a UVO (UV light and Ozone gas) cleaner for 15 min prior to stamping.

2.2.2.3 Alternate coverslip preparation

As an alternate to the culture dishes, we prepared 40mm PDMS spin-coated coverslips with μCP of patterned PDL for use in a Bioptechs closed chamber system (Bioptechs, FCS2/FCS3) live imaging chamber specifically designed for these size coverslips. Coverslips were prepared in the same manner as the 25mm ones described in 2.2.2.2. On these coverslips, cells were allowed to attach and grow for 24 h prior to transfer into the chamber followed by 12 h of live imaging. This system was implemented because it allows for the objective to access a greater area of the coverslip, which included the entire stamped area.

2.2.2.4 Microcontact Printing of Poly-D-lysine

Microcontact printing of poly-D-lysine was done on culture dishes or coverslips (section 2.2.2.2 and 2.2.2.3). Stamps were premade and generously provided by Dr. Feinberg's lab at Carnegie Mellon University. The pattern used was 20 µm thick lines of PDL at 30 μm intervals. PDMS stamps were sonicated pattern side up in 10 % W/V Sodium Dodecyl Sulfate (SDS) for 30 min (SDS was used as release layer to enhance transfer of PDL from stamp to coverslip (60)), then transferred immediately to a sterile culture hood. Stamps were dried with a nitrogen air gun and coated with 200 µL of 200 μg/mL PDL. Once pipetted onto stamp, maximum coverage was ensured by gently dragging the edge of the pipette tip over the PDL, using the surface tension to expand droplet to each corner of the stamp. Stamps with PDL were kept under sterile conditions at room temperature for 1 h t o allow adequate "inking". After this incubation period, stamps were rinsed twice in sterile diH$_2$O and dried with nitrogen air gun. Stamps were then inverted onto PDMS-coated coverslips directly over the center hold drilled into the culture dish and gently tapped using sterile forceps to ensure complete contact. After 5 min, they were gently

removed without disrupting the pattern, and either re-inked or stored for future use. Stamped dishes were filled with sterile diH$_2$O, wrapped in Parafilm and stored at +4 ºC until use.

2.2.2.5 Cell Culture and Live Imaging

DRG neurons were dissected and prepared for culture as described previously (see **2.1.2.2 Neuronal Cultures**). Prior to plating, cells were run through a 50 µm cell strainer to remove any connective tissue debris. Just prior to use, µCP dishes were treated with 1 % Pluronics F-27 solution for 5 min followed by 3 washes with sterile diH$_2$O. Then all fluids were removed and 200 µL of strained cells were plated on the µCP dishes, incubated for 2 h to allow attachment, and then filled with culture media and incubated for 10 h (37 ºC, 5 % CO$_2$) to allow initial growth to occur. Cultures were then treated with 25 mM HEPES and imaged using Differential Contrast Imaging (DIC) on a Nikon T2 Live cell imaging system with an atmospheric and temperature-controlled stage (37 ˚C, 5 % CO$_2$) using a Nikon CFI Plan Fluor objective (40 x oil, NA 1.3) (for schematic of set-up see Figure 9). Fifteen different XY coordinates were taken at each time point, 10 msec exposure time, 10 min time between acquisitions, for a duration of 12 h. Medium containing either aLam or nLam was added at the 1 h time point. Images were acquired using a Photometrix camera and videos were collected and processed using NIS Elements 4.0 software.
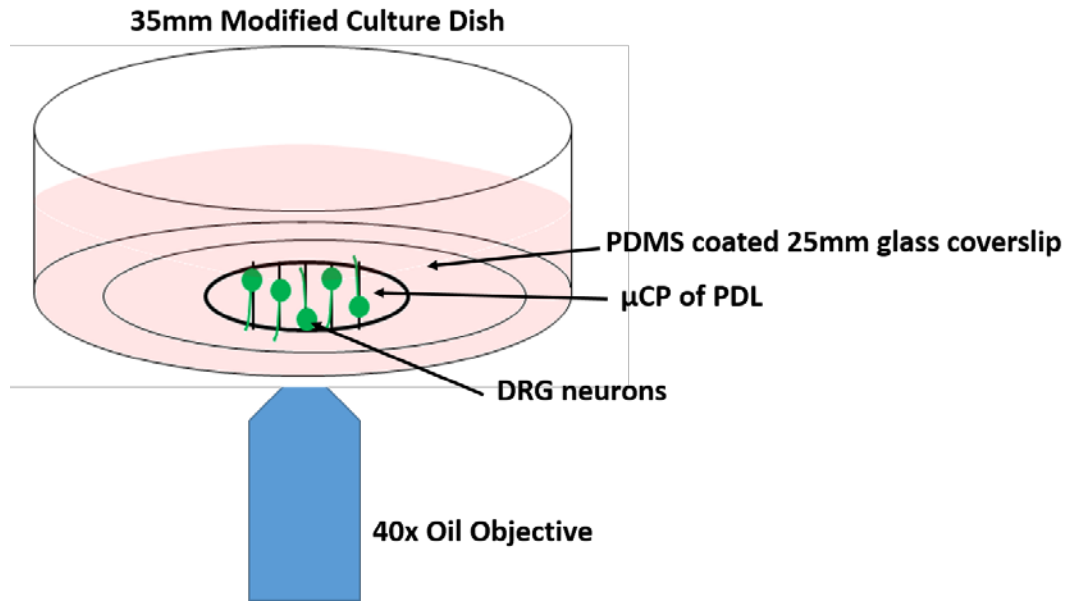
Figure 9 Schematic of modified culture dish

2.2.2.6 Statistical Analysis

Factorial ANOVA is used to evaluate growth speed, neurite length, and number of neuron-glia interactions between aLam and nLam groups. Differences between groups were considered significant at $p < 0.05$.

2.2.3   Results

2.2.3.1 Microcontact Printing with SDS release layer is an efficient way of creating patterned PDL for axonal guidance in culture

Prior to live imaging, stamped dishes were evaluated with and without cultured cells and stained for visualization. Results indicated that stamping technique was: a) effectively transferring PDL in the desired pattern, and b) the patterned lines had sufficient width to allow for cell attachment and directional growth. Figure 10 illustrates a stamped pattern with and without cell attachment.

The PDL concentration of 200 µg/mL proved to be optimal for stamping and the 20 µm width of the PDL pattern allowed for cell attachment and directional outgrowth.
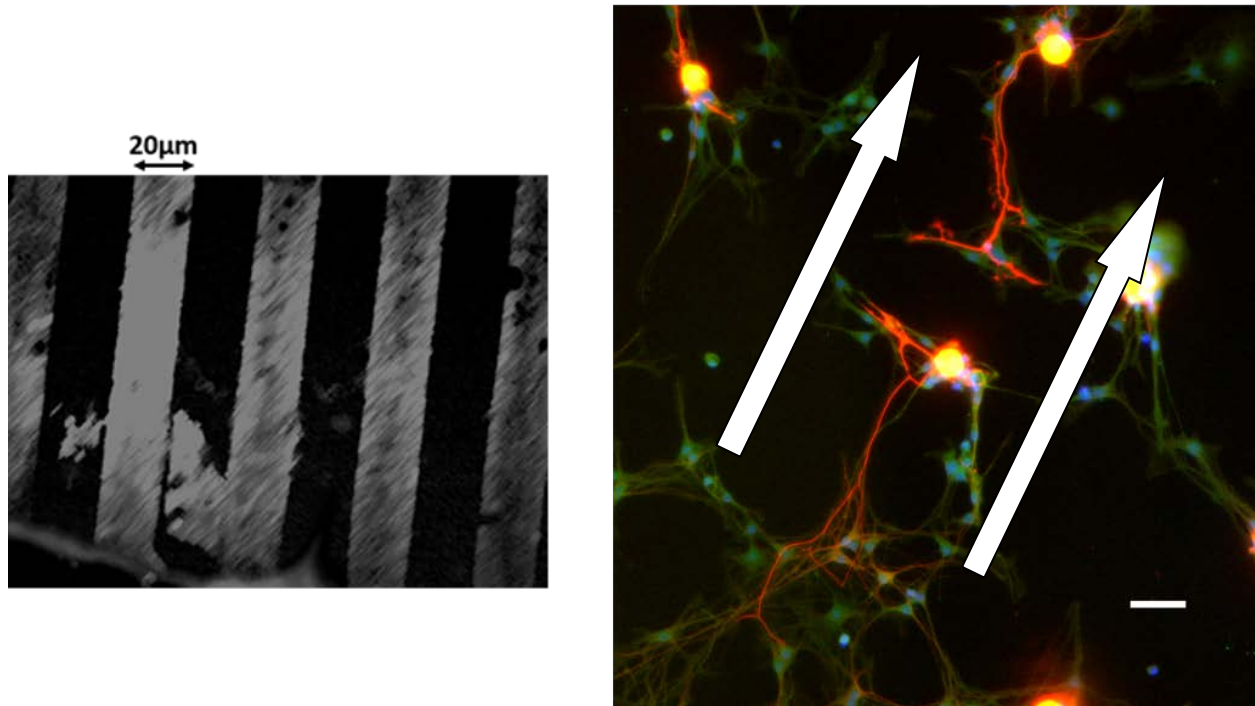
Figure 10 Image of poly-D-lysine stamp on PDMS coated coverslip. (A) Coverslip without cells (goat α mouse AF 555; 1:500); (B) with neurons attached (βIII tubulin(red)/S100(green)/DAPI(blue)), arrows denote direction of pattern, scale bar=50µm. Note: Images artificially brightened for better visualization.

2.2.3.2 Neurons did not adhere strongly enough for live imaging outgrowth assessment

When our cultures were transported for live imaging, there was a noticeable trend that the cells were not remaining adherent and there were significantly less cells observed under live imaging conditions than initially observed under normal culture conditions. Cells that remained

attached did not achieve significant levels of outgrowth regardless of whether we implemented

modified culture dishes (Section 2.2.2.2) or alternative stamping (Section 2.2.2.3) methods

(Figure 11).
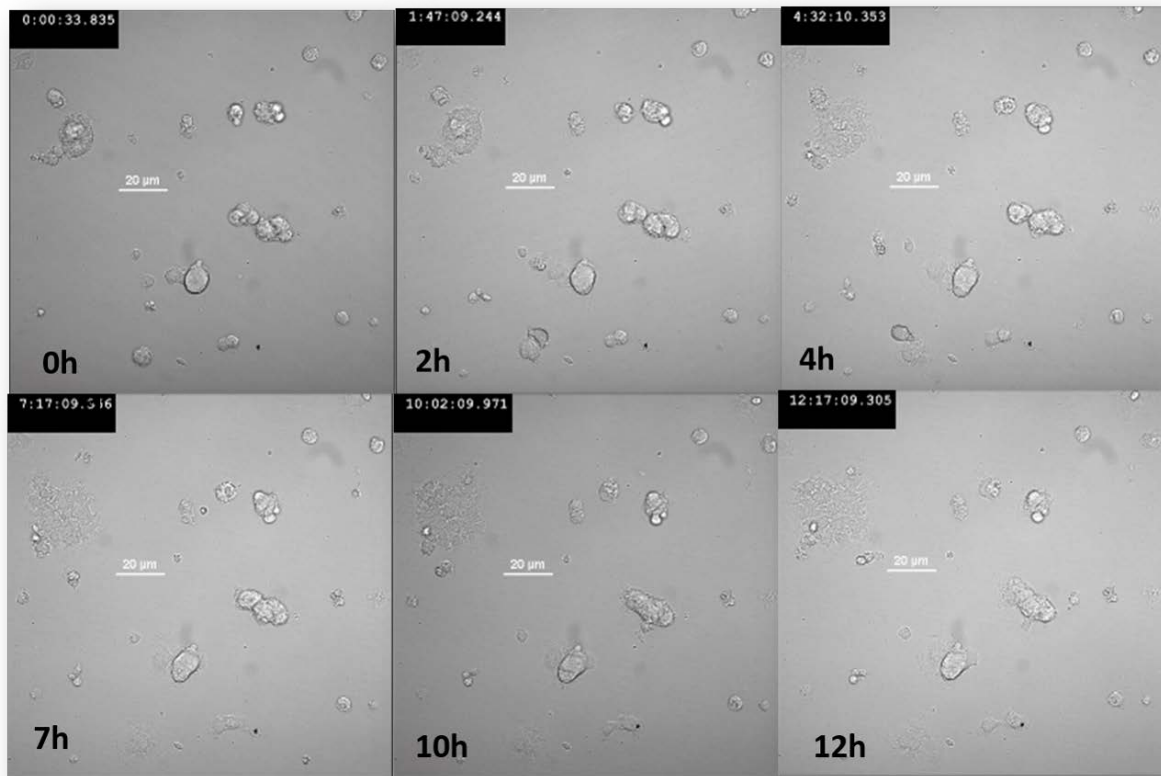
Figure 11-Live Imaging aLam. 12h of live imaging on modified culture dish with stamped PDL revealed little adhesion and movement (either growth or direction).

2.2.4 Discussion and future studies

Our results here suggest that microcontact printing holds potential for directed neuronal cell grow using a growth neutral substrate (PDL) in culture. DRG neurons and glial cells were able to adhere and neurons extended neurites along stamped PDL. However, some aspects of this method could benefit from further optimization. D istance between stamped lines may be extended to the point that glia cells are unable to bridge them. Using the current pattern, glia appear to have formed bridges between substrate lines, which allowed neurites to grow both in phase with the stamped substrate, as well as perpendicular to it.

When attempting to translate from still post-fixation figures to live imagine, we made some interesting observations. Relatively few viable cells remained on the pattern. O riginal modified imaging dishes restricted the area of focus so that the objective had access to only a small percentage of the total stamped area. This was our initial motivation for utilizing the alternative coverslip stamping preparation, which allowed the objective to capture the entirety of the stamp. T herefore we were able to determine that cells were consistently not achieving a sufficient level of adherence required for live imaging at any part of the stamped substrate. Increasing the width of stamped lines from 20μm to 50μm may encourage greater cell adhesion to the pattern. In spite of the limited overall adherence, cells that were captured, using either of our methods (dishes or Bioptechs), remained viable for the entire 12h i maging period. T his finding shows that we can successfully image neurons over this period of time using the current protocol without loss of viability.

In order to assess growth dynamics associated with aLam treatment in culture, some future design steps may be considered, 1) evaluate different stamped patterns including patterns with wider substrate lanes (some DRG cell bodies can reach up t o 50μm in diameter) for

stronger soma attachment and wider lanes between growth lane to discourage glial bridge formation; 2) optimize timing of imaging so that cells have additional time for stronger adherence and outgrowth initiation and implement measures to minimize movement of dishes during transport that could initiate sheer force, breaking cell adhesion bonds. Although 12 h was calculated as the optimal imaging time in order to visualize some initial outgrowth to track, this was optimized using PDL coated, not stamped dishes, stamped dished appear to require addition time to achieve similar level of outgrowth. With the restricted attachment substrate, neurons appear to interact less with one another as well as with glial cells. We could potentially overcome some of this by culturing the neurons utilizing a higher plating density. Overall, this technique shows promise for analyzing real-time growth dynamics of cultured adult neurons over long periods of time.

3.0   TESTING OF ACIDIC LAMININ FOR NERVOUS TISSUE REPAIR

Our data from chapter two suggests that DRG neurons exposed to aLam *in vitro* exhibit increased growth competence resulting in longer neurites than those in nLam or culture medium only without laminin polymers. In this chapter, we will test whether or not aLam has similar effects on neurons *in vivo* and whether this would result in increased repair. DRG neurons *in vivo* are referred to as 'pseudounipolar cells' because they have a single axon that splits shortly after leaving the cell body with one branch projecting out into the periphery through the peripheral nerve while the other branch projects through the dorsal root towards the spinal cord where they either terminate in the grey matter of the segment of entry or course through the dorsal columns towards the dorsal column nuclei in the brainstem. To test whether the *in vitro* actions of aLam can be translated into *in vivo* nervous tissue repair, we have elected two models of nervous tissue injury that represent each of the two environments, PNS and CNS, in which the bipolar DRG neurons extend their axons. It is well known from the literature that these two environments differ in how they respond to an injury and to what degree they support axonal re-growth. By considering both types of environments we can more accurately evaluate the potential of aLam as a treatment for nervous tissue repair. Within these two environments, we chose clinically relevant models of 'closed' injuries that would allow injection of the laminin polymers. In the periphery, we utilized a moderate crush injury model (Seddon classification level

axonotmesis/Sunderland forth degree-epineurium intact) (49, 50). C entrally, we utilized a contusion injury, which is the most common mechanism of SCI in humans (54).

For both *in vivo* studies conducted, all animal care and procedures were done in accordance with approved guidelines set by the National Institutes of Health and the United States Department of Agriculture and monitored by the University of Pittsburgh Institutional Animal Care and Use Committee, protocol approval #12050540. A ll rats were housed within a double-barrier animal facility with 12 h/12 h light/dark cycles and continuous access to fresh air, food, and water.

3.1   ACIDIC LAMININ FOR PERIPHERAL NERVE REPAIR

3.1.1   Introduction

The peripheral nervous system is defined as the nerves and ganglia that lie outside of the brain and spinal cord. This environment differs from the CNS in both its glial population (Schwann cells and Satellite cells versus astrocytes, oligodendrocytes, and microglia) and access to blood supply and nutrient (lack of a blood - peripheral nerve - barrier versus a blood - brain (spinal cord) - barrier). S chwann cells play an important role in the relative larger regenerative competence of damaged axons in the PNS (61). Upon injury, Schwann cells dedifferentiate into nonmyelinating cells that, along with macrophages, clean up damaged myelin and other cellular debris, produce ECM, secrete numerous growth factors, and form Bands of Bungner, which all together create conducive regeneration pathways for severed axons. Following successful axon regeneration, Schwann cells differentiate back to their mature state and myelinate the new

processes (61). One of the ECM components produced by Schwann cells is laminin which in the PNS plays an essential part in the regeneration response. It was shown that in mice in which Schwann cells were genetically altered to not produce and secrete laminin the regeneration response was significantly impaired following a sciatic crush injury(62). DRG neurons express α1 and α3 laminin-binding integrins at the surface of their cell bodies and growth cones in culture as well *in vivo* (Figure 10).
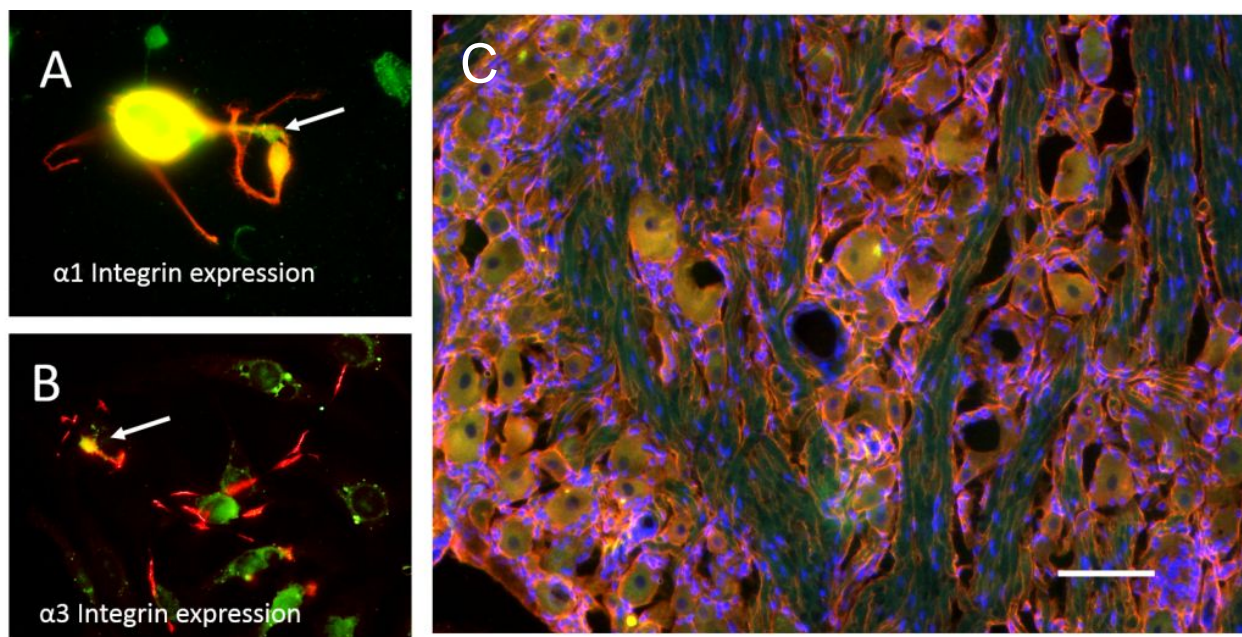
Figure 12 Integrin Expression of DRG cells in culture and tissue. A) α1 integrin expression in culture at the cell body and growth cone (arrow) *βtubulinIII (red), alpha1 (CD49a) (green)*. B) α3 integrin expression in culture at the cell body and growth cone (arrow). *βtubulinIII (red), alpha3(CD49c) (green).* C. Integrin expression in DRG tissue slice (*CD49a (red), CD49c (green), DAPI (blue); Scale bar=100µm*)

Combined with our *in vitro* findings, this information implies that aLam could support axon regeneration following a moderate crush injury of the peripheral nerve. Injuries to the peripheral nervous system are common and can have a devastating impact on a person's daily life. One possible treatment is to promote and/or enhance axon regeneration using extrinsic signalling cues administered following injury, Using Seddon's method of nerve damage characterization, we focus on a n injury model of axonotmesis because it represents an injury that typically requires some type of intervention for recovery, but does not require an implantable guidance conduit because the epineurium remains intact (49). This is, therefore, an ideal injury model to test an injectable signaling molecule such as aLam. In the study described in the first part of this Chapter, we will test the **hypothesis** that *aLam promotes axonal regeneration and functional recovery in a clinically relevant model of peroneal nerve crush.*

3.1.2 Materials and Methods

To test the regenerative capability of aLam *in vivo*, we injected aLam polymers into the crushed peripheral nerve of adult rats and evaluated motor and sensory function over a course of ten weeks post injury and injection. The rats were then perfusion fixed and the peripheral nerve and DRGs prepared for histological assessment of axonal regeneration.

3.1.2.1 Surgical Procedures

Female adult Sprague Dawley rats (225-250g, n=21; Charles River Laboratory, Wilmington, MA USA) were anaesthetized using intraperitoneal injection of a cocktail of ketamine (60 mg/kg; Butlerschein, Dublin, OH USA) and Dexdomitor (0.5mg/kg; Pfizer, New York, NY USA)(7).

The right hind limbs was shaved and cleaned with 70% ethanol followed by Betadine® scrub (Figure 11A), the thigh muscles were exposed and separated to reveal the peroneal nerve and a 30 sec crush was made using #5 fine forceps (Fine Science Tool, Foster City, CA). The nerve was consistently crushed where it passed over the tendon, which was used as an anatomical marker to ensure consistency between rats and for nerve dissection at the end of the functional testing (Figure 11B and C). The completeness of the crush was confirmed visually by the presence of a translucent band (Figure 11D, circled). Two days after the crush, animals were randomly assigned into one of three groups (n=7/group) and their injured nerve was re-exposed and 3 µL of either aLam, nLam or PBS was injected into the injury site using a 10 µL Hamilton syringe fitted with a pulled glass needle. The investigator performing the injections was blinded to the treatment groups. Starting 14 d ays post injection (dpi), gait was tested using the DigiGait™ Image Analysis System until 70 dpi. T he investigators conducting the behavioral assessments were blinded to experimental group.

After final behavioral testing, animals were anesthetized as described above and nerves were traced using a 3 µL injection of Cholera Toxin B subunit (CTB; 1% CTB in sterile diH$_2$O; List Biological Laboratories, Campbell, USA) 10 mm distal to the crush site (63).
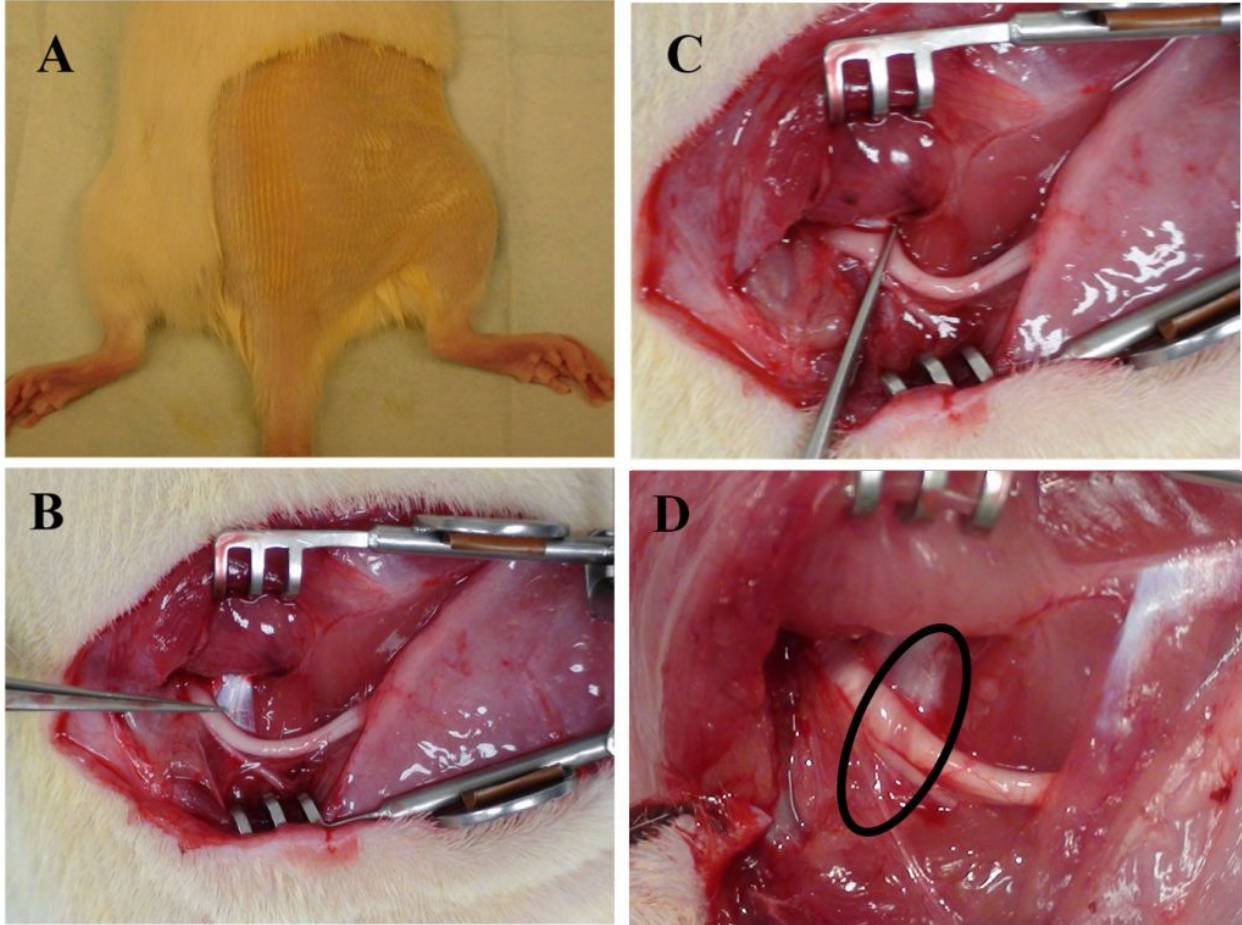
Figure 13 Peroneal Nerve Injury. A. Right hind limb prepped for surgery. B. Muscles separated to reveal peroneal nerve. Forceps indicated tendon used as anatomical marker of injury. C. 30 sec crush injury at anatomical marker with fine forceps. D. Circled area denotes translucent band indicative of axonotmesis crush injury.

3.1.2.2 Post-Surgery Procedures

Antisedan (1.5 mg/kg; Pfizer) was injected subcutaneously to reverse the effects of dexdomitor. An intramuscular injection of gentamicin (6 mg/kg; VWR), a subcutaneous injection of Rimadyl (5 mg/kg; Pfizer), and a subcutaneous Ringer's solution (5 mL) were administered daily for two days post injury. After injection, all rats received three additional days of Rimadyl (5 mg/kg, 1x

daily). All rats were monitored daily throughout the course of experiment. Autophagia of the injured limb may occur with this type of peripheral nerve crush. At the first sign of autophagia, rats were treated with topical lidocaine, Zymox® with 1 % hydrocortisone, and bitter spray to heal the wounds and discourage future chewing. All animals were supplied daily with paper huts to chew. Rats were perfusion fixed with 0.01 M PBS followed by 4 % Paraformaldehyde (PFA) at 11 weeks post injury.

3.1.2.3 Motor Function Assessment

The DigiGait^{TM} Image Analysis System (Mouse Specifics, Framingham, MA, USA) was employed to investigate gait (Figure 16). P reliminary study revealed the importance of acclimating rats to the DigiGait^{TM} prior to data collection. F or acclimation, rats were first introduced into the DigiGait^{TM} chamber with the treadmill and lights off. Then, for 8 m in for four days, the rats were placed on the treadmill at a starting speed of 3 cm/sec which was slowly increased to the target speed of 20 c m/sec on the fourth day, at which time baseline measurements were recorded. The target treadmill speed of 20 cm/sec (zero degree incline) was chosen because it requires continuous walking (no running) for all rats, but it is not so laborious that injury prevents successful participation for most animals. Rats that did not walk at the target speed were excluded from the study. The complete behavioral testing schedule was: 1 day prior to surgery (baseline), 14 dpi, then weekly up to 42 dpi and bi-weekly from 42-70 dpi. The main motor outcome measure was Peroneal Function Index (PFI).
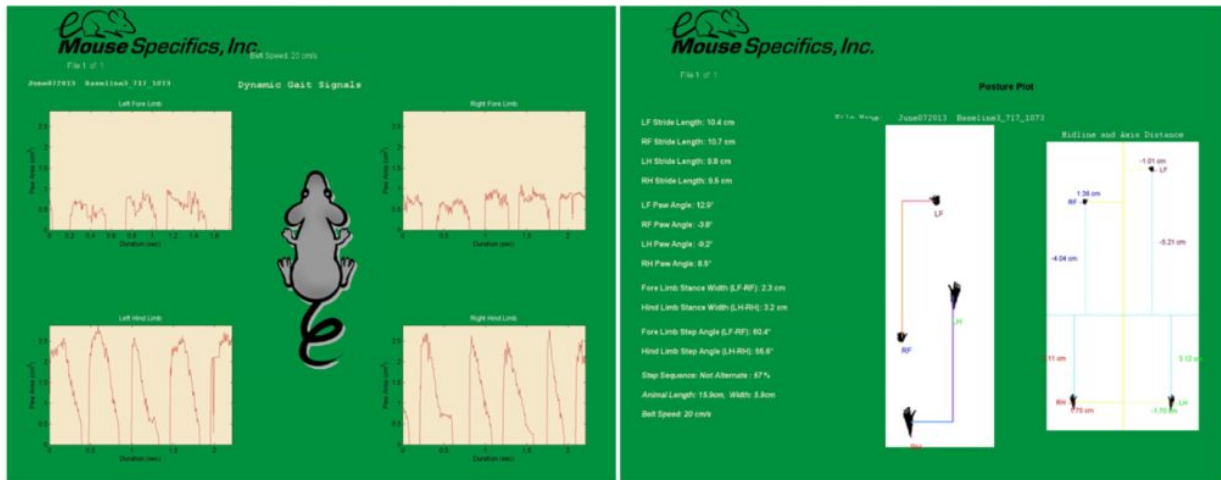
Figure 14 DigiGait® Automated Treadmill walking device and software to detect differences in gait.

Top: Image of rat treadmill walking in chamber, bottom left: dynamic paw area and gait signal plots, bottom right: posture plots**.**

3.1.2.4 Immunohystochemistry

Following the 70 dpi behavioral measures, animals were anesthetized and transcardially perfused with 300 mL of 0.01M PBS followed by 400 mL of 4 % paraformaldehyde (PFA). A 5 mm-long piece of the peroneal nerve centered on the crush site and the proximally adjacent 5 mm-long section were dissected and post-fixed overnight in 4 % PFA, followed by treatment with 30 % sucrose solution and storage at +4 ºC. Then, 15 μm thick longitudinal sections were

cut in five series using a cryostat microtome at -24 ºC and mounted on positively charged microscope slides. Nonspecific binding sites were blocked using 0.01M PBS with 5 % Normal Goat Serum (NGS) and 0.03 % Triton blocking solution at room temperature for 1h. To evaluate nerve regeneration, sections were incubated with anti-neurofiliament-heavy type (NF-h) antibodies (1:250, Millipore AB1991) at 1 h at room temperature followed by overnight at +4 ºC. Neurofilament is a major component of the neuronal cytoskeleton, mainly found in the axon where it provides support and participates in axonal transport. After washing with 0.01 M PBS, secondary antibody reaction was initiated using AlexaFluor 488 fluorescent antibodies against rabbit (1:1000, Molecular Probes) for 1 h at room temperature followed by 3x washing, DAPI counterstain, and covering with a glass slip using anti-fade fluorescent mounting media (Dako, #S3023, Carpenteria, CA, USA). The number and size of NF-h positive axons crossing the crush site were determined using a Zeiss Axio Observer inverted fluorescent microscope with Zeiss Plan Apochromat objective (20x air, NA 0.8) and quantified using ImageJ (58).

3.1.2.5 Semi-thin nerve sections

A 3 mm long piece of the peroneal nerve just distal to the crush was removed and post-fixed in 2.5 % gluteraldehyde overnight in 4 ºC for semi-thin sections. Tissue was then rinsed three times in PBS and then penetrated with OsO_4 overnight. After washing, the tissue was processed using serial drying with increasing concentrations of ethanol from 30 - 100 %. Tissue was then treated with propylene oxide (PO), combination PO:Epon® (3:1, 1:1, 1:3), 100 % Epon® and embedded in silicone molds with Epon® resin. Following 24 h curing at 37 ºC and 48 h at 65 ºC, cross sections of nerve were cut using a diamond knife at a thickness of 400 nm and stained with toluidine blue for myelin analysis and quantification.

3.1.2.6 Myelin Quantification

Toluidine blue (tolonium chloride) is a staining solution that at high pH will bind to nucleic acid and proteins. The alkaline form is used here to delineate structural components of our semi-thin sections in order to quantify total myelinated fibers in cross sections of nerves just distal to the crush. Preliminary data showed that while there were significant differences found when comparing more proximal sections of the nerve to those within the injury site, there was no difference in total area of myelination, size or number of myelinated fibers when comparing within the injury site to the adjacent distal section, therefore numbers here will be taken as representative of re-myelination across the injury. Total area and number of myelinated fibers were quantified using ImageJ (58) particle analyzer and averaged per experimental group.

3.1.2.7 Statistical Analysis

Statistical analyses were performed using SPSS statistical software package (SPSS version 21, IBM). One-way ANOVA with Tukey's post hoc was used to measure histological differences between groups. Repeated measures ANOVA with Tukey's post hoc were used to evaluate differences in behavioral measures. Differences were considered significant at $p \leq 0.05$.

3.1.3   Results

3.1.3.1 Laminin treatment resulted in decreased autophagia

Autophagia was characterized under two categories; early (before injection) and late (at least one week post injection). If any blood was visible on toenails or lacerations/ulcers on the right hindpaw it was marked as autophagia. Equal numbers of early autophagia occurred throughout

groups (n=2/7 for each group). For late autophagia, the incidence was lowest in aLam treated rats (n=1/7) compared to nLam treated rats (n=2/7) or PBS treated rats (n=3/7).

3.1.3.2 aLam treatment increased compliance for treadmill walking

Prior to injury, baseline measures were taken from all animals and only those with perfect compliance were selected for the study. Following crush injury, the group with aLam treatment remained at 100% compliance for treadmill walking at all behavioral time points. In the nLam treatment group some animals refused to walk at the target speed at 28 and 70 dpi. In the PBS treatment group, there were several rats that refused to walk at the target speed at each time point after 14 dpi (Figure 13).
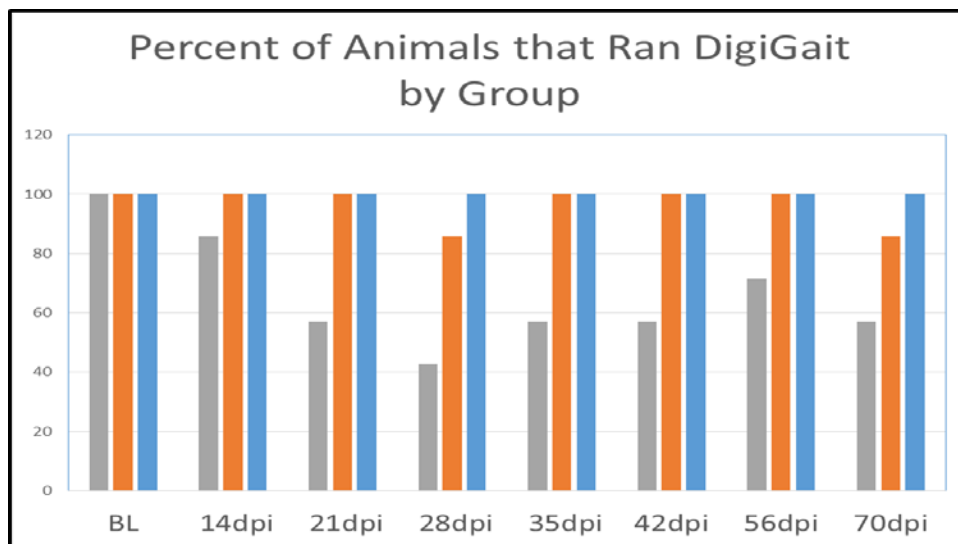
Figure 15 Compliance for Automated Treadmill Walking. aLam group achieved 100% compliance for treadmill walking at every time point *(aLam=blue, nLam=orange, PBS=grey)*

3.1.3.3 No difference in peroneal function index at 70 dpi

Repeated Measures ANOVA was conducted on standardized PFI data (timepoint-baseline) and no significant effect of group was found (p=0.07). Nerve function in the aLam and nLam groups was similar (p=0.8) and both groups trended towards significance from the PBS group (p=0.07), but did not reach the set value. Results from PFI analysis and example of DigiGait hindpaw area graphs are depicted in Figure 14.
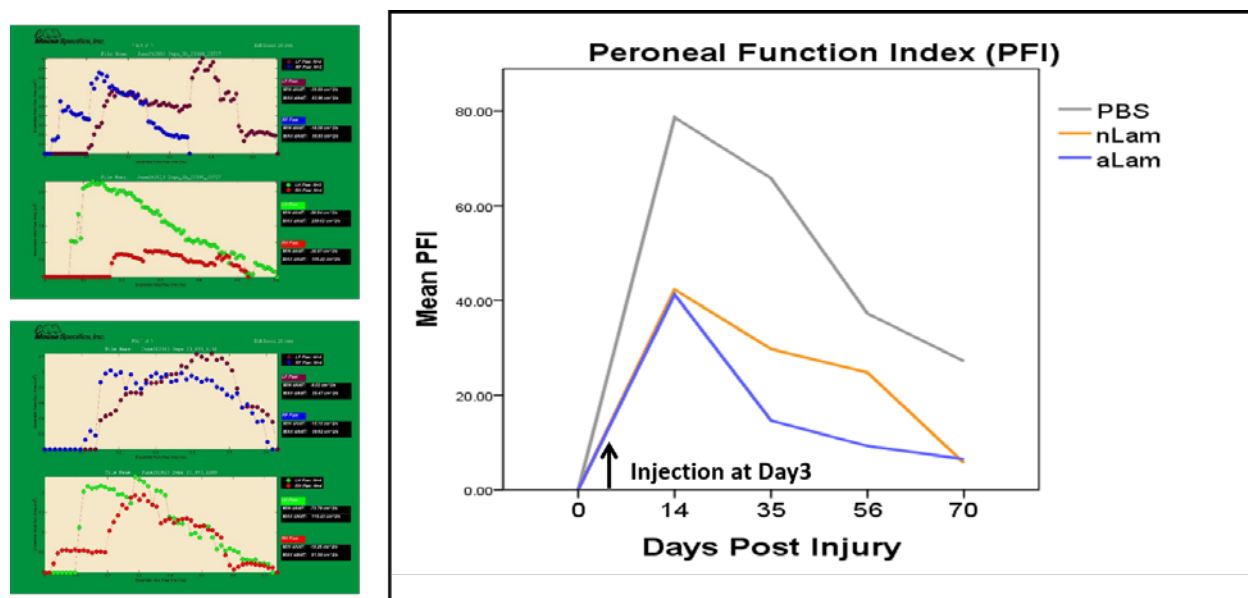
Figure 16-Peroneal Function Index. *Left:* DigiGait paw area graphs. Top graphs (blue/purple dots) represent forepaws and bottom graphs (green/red dots) represent hindpaw. Top pair is representative of 14 dpi and bottom pair of 70 dpi. Bottom right hindpaw (red) has regained area indicative of functional recovery. *Right:* Standardized PFI graph shows loss and return of function of right hindpaw in all groups along the course of the study (aLam(n=5), nLam(n=6), PBS (n=3)).

3.1.3.4 aLam treatment increased the number of large diameter axons at 70dpi

NF-h staining was used to determine the amount of axon regeneration/sprouting across the injury site. We found significantly more large diameter axons in the aLam group than in the nLam or PBS group ($p<0.05$). There were no differences found in total number of fibers or total area of NF-h staining ($p>0.05$) (Figure 15).
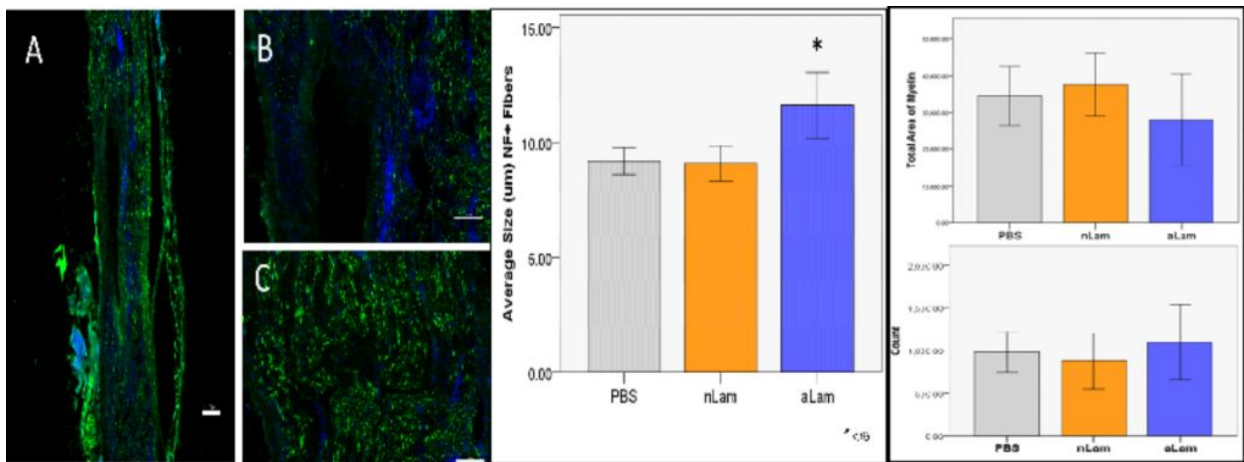
Figure 17 Peroneal Nerve Regeneration. Image: Example of a crushed peripheral nerve 10 weeks post-injury (A), at (B) and away (C) from the crushed site *(NF-h (green) and DAPI (blue), Scale bar= 250 μm on A and 50 μm on B and C).* Graphs: Significantly more large diameter axons found in aLam treatment group than nLam or PBS control at 70dpi (ANOVA, $p<.05$). Overall total number or area of NF-h positive axons did not differ between groups.

3.1.3.5 No difference in myelination of nerve between groups

Myelin was quantified using the semi-thin sections stained with toluidine blue. Five sections per animal were quantified and averaged. Analysis showed no difference in total area or number of myelinated fibers between groups (Figure 16).
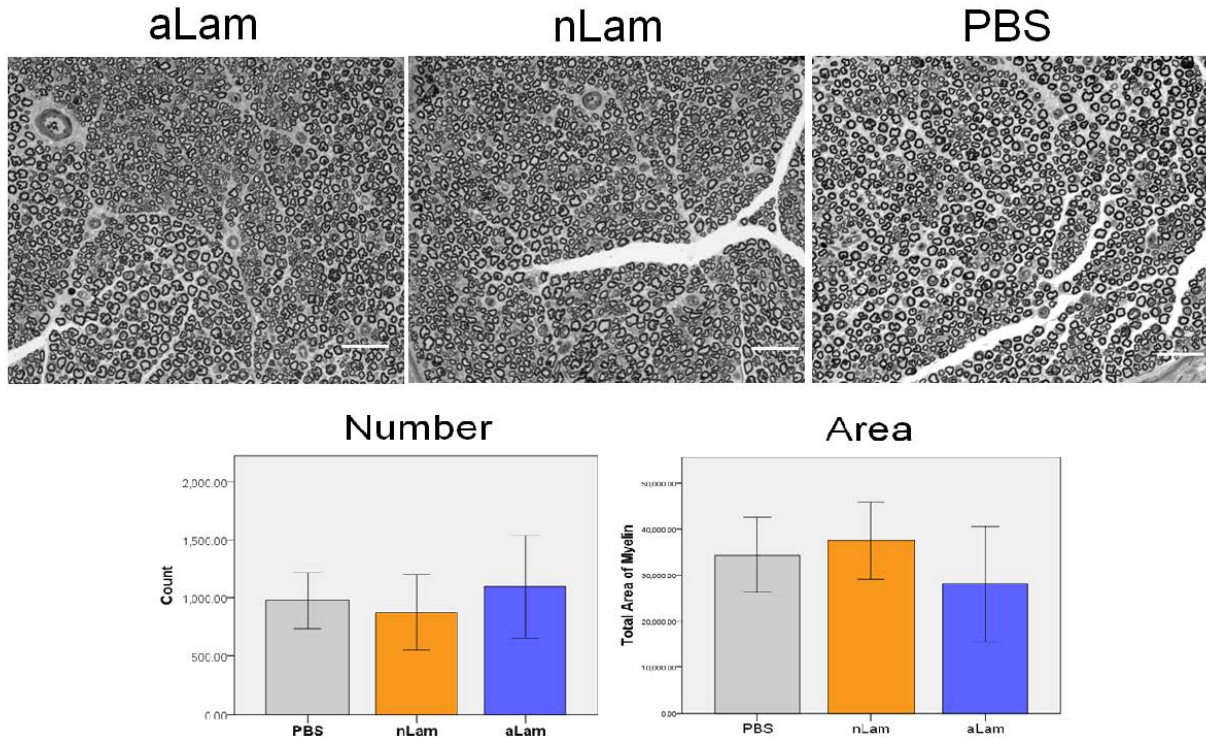
Figure 18 Myelin Quantification. Top: Semi-thin plastic sections stained with toluidine blue (Scale bar= 50μm). Bottom: No difference observed in number of myelinated fibers or total area of myelin (PBS (grey), nLam (orange), aLam (blue), p>.05)

3.1.4 Discussion

Our *in vitro* studies described in Chapter 2 demonstrated that aLam can act as a signaling molecule promoting neurite growth from DRG neurons *in vitro*. In the present study we investigated the repair potential of aLam using a clinically relevant *in vivo* model of peripheral nerve damage. Our findings partially supported our hypothesis showing that aLam treatment

resulted in enhanced axon regeneration. We did not observe enhanced functional recovery. The data suggests that 1) aLam increases compliance on treadmill running after injury; 2) aLam decreases autophagia, a common occurrence following PNI; 3) aLam was associated with significant increase in large diameter axons across the crush; 4) there were no significant differences in area of myelination or number of myelinated axons; 5) there were no significant differences in motor recovery as measured by the peroneal function index. Together these results support the notion that aLam has potential for treatment as an injectable signaling molecule. It showed increased biocompatibility and no additional damage or discomfort was observed in the rats. In fact, the decreased autophagia in the aLam group can be interpreted that aLam treatment alleviated discomfort normally associated with this type of injury. Further research will be needed to elucidate aLam's role in these findings.

Although there were no overall significant differences in PFI, there appeared to be a trend towards earlier recovery in the polymerized laminin treatment groups. Due to the low number of compliant controls in the behavioral evaluation, it is difficult to say whether additional data would have further separated these findings into significance. One could postulate that those animals which complied with the task demands represented only the highest functioning controls, whereas the aLam group data, with 100 % task compliance, was the most accurate representation of the three experimental groups. If one were to include lower functioning controls, this difference may become more apparent, but additional studies, employing perhaps a less demanding, but equally sensitive behavioral measure, are needed to test this theory.

One caveat of this model is that all groups showed improvement in motor function by 70 dpi, at which point all histological data was collected and analyzed. The similar functional outcomes were in agreement with the lack of differences between groups in total number of

axons and myelination. Peripheral axons exhibit a relative high intrinsic ability to grow and can reach growth speeds of 5 mm/week. Thus, it is possible that we missed the window at which we could have detected differences in total number of regenerated fibers. Evaluation of histology at earlier time points after injury/treatment could provide additional information about the true potential of aLam treatment to promote axon regeneration and functional recovery after PNI. Alternatively, a more severe injury could provide additional data, but this also may further incapacitate our control group for behavioral measures.

A clinically significant finding in our study is aLam's effect on autophagia. Autophagia is a common occurrence in peripheral nerve injury in rats and can lead to devastating self-mutilations. T he fact that aLam all but abolished this response underscores its potential for further development as a therapeutic for PNI.

3.2   ACIDIC LAMININ FOR SPINAL CORD REPAIR

3.2.1 Introduction

The central nervous system (CNS) consists of the brain and spinal cord, which are physically separated from the rest of the body through the blood - brain/spinal cord – barrier. This barrier presents a unique challenge when developing systemically delivered treatments for repair. Due to the closed structure of the CNS, developing injectable treatments with minimally invasive delivery may be preferable.   Following traumatic injury, adult CNS neurons, although intrinsically capable of regeneration (64), do not spontaneously regenerate damaged axons.

Strategies that promote axonal regeneration or plasticity after CNS injury are necessary for recovering disrupted motor and sensory circuits and reinstating functional flow of information between the brain and periphery. In order for this to occur there are many obstacles to axon growth that one must overcome, including an abundance of inhibitory molecules, lack of growth-promoting molecules and loss of matrix substrate. Laminin has been shown to be involved in growth promotion (25, 62) and as a guidance matrix (31, 65, 66) during development and after injury, making it an interesting candidate treatment for repair. Our previous studies suggest 1) that aLam acts as an axon growth-promoting molecule *in vitro*, 2) aLam signals its growth effects through α1 and or α3 integrins, and 3) aLam can be employed as an injectable treatment to elicit growth responses in the damaged peripheral nerve. In the study described in this chapter, we will test the therapeutic potential of aLam for damaged central nervous tissue utilizing a clinically relevant model of spinal cord contusion injury.

Our previous studies showed that polymerized laminin requires α1 and α3 integrin receptors to initiate growth signaling responses. These laminin polymer-binding integrins are also mostly absent in healthy, uninjured, spinal cord tissue (Figure 19, A). Following a contusive SCI, there is a significant increase in both α1 and α3 integrin receptors at and around the injury site (Figure 19, B). This increase is at least in part attributed to an increase in expression on spinal motor neurons, which show expression of one or both types of integrins (Figure 19, C (arrows)).
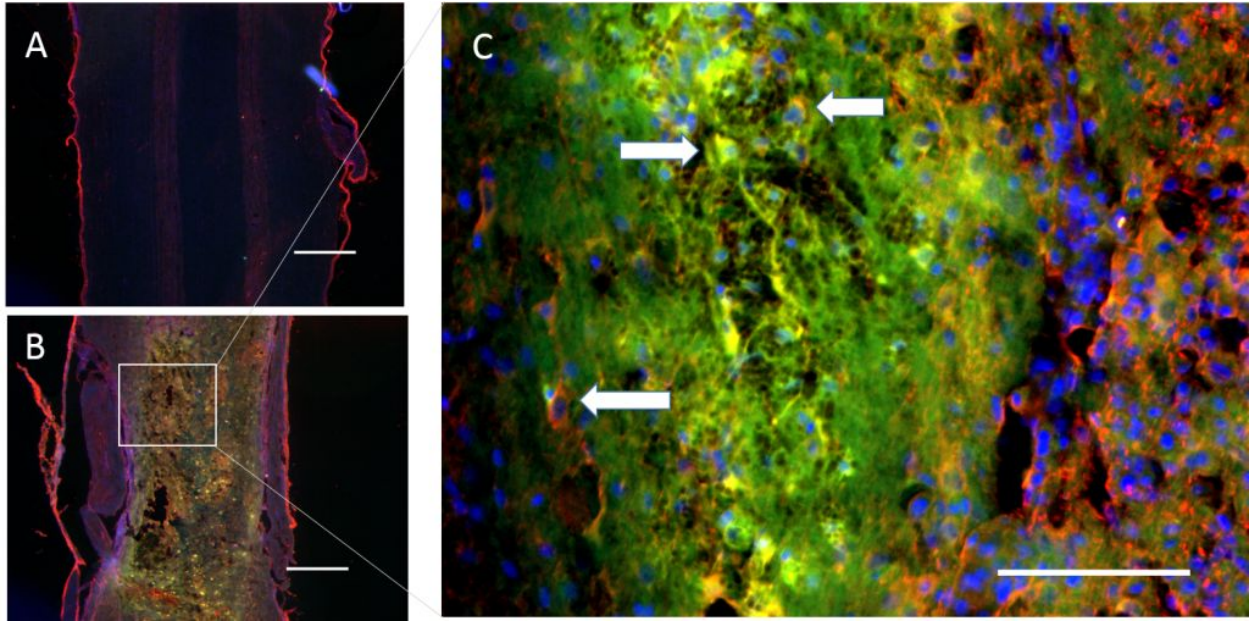
Figure 19 Integrin Expression after SCI. A. α1 (red) and α3 (green) integrin expression in uninjured, healthy spinal cord thoracic segment. B. α1 (red) and α3 (green) integrin expression at three days post 200kDyne contusion injury (T9 spinal segment). C. Increased magnification of injury site to show expression increase is (in part) due to an increase in expression of one (bottom arrow) or both (top arrows) integrins to varying degrees in motor neurons. Note: Same camera and microscope settings used for A and B

In this chapter, we will test the **hypothesis** that *aLam promotes axonal growth in a contusion model of spinal cord injury thereby improving functional recovery.*

3.2.2   Materials and Methods

3.2.2.1 Surgical Procedures

A model of adult rat spinal cord contusion (7, 67, 68) was used to test axonal regenerative effects of aLam. Female adult Sprague Dawley rats (225-250 g, n = 30; Charles River Laboratory,

Wilmington, MA USA) were anaesthetized using intraperitoneal injection of a cocktail of ketamine (60 mg/kg; Butlerschein, Dublin, OH USA) and Dexdomitor (0.5 mg/kg; Pfizer, New York, NY USA) (7). The dorsal surfaces of animals were shaved and then cleaned with 70 % ethanol followed by Betadine® scrub, the tenth thoracic spinal cord segment was exposed via laminectomy and contused using a force of 200 kDyne (Infinite Horizon IH-0400 impactor; Precision Systems and Instrumentation, LLC, Versailles, KY USA) (69) (Figure 20). The injury site was rinsed with sterile saline containing 0.1 % gentamicin (VWR, Radnor, PA), the muscles were sutured in layers and the skin was closed with Michel wound clips (Find Science Tools, Foster City, CA USA). Rats were included in the study based on receiving an impact within 5 % of the intended force and a Basso-Beattie-Bresnahan (BBB) (70, 71) score of ≤ 1 at day 1 and $\leq$ 5 at day 3 post-contusion. Three days post injury, which was previously identified as an optimal time point for therapeutic intervention (67), rats were randomized, sedated and 5 µL of either aLam (50 µg/mL), nLam (50 µg/mL) or 0.01 M PBS in was injected into the epicenter of the contusion by an investigator blinded to the treatment administered (Figure 20).
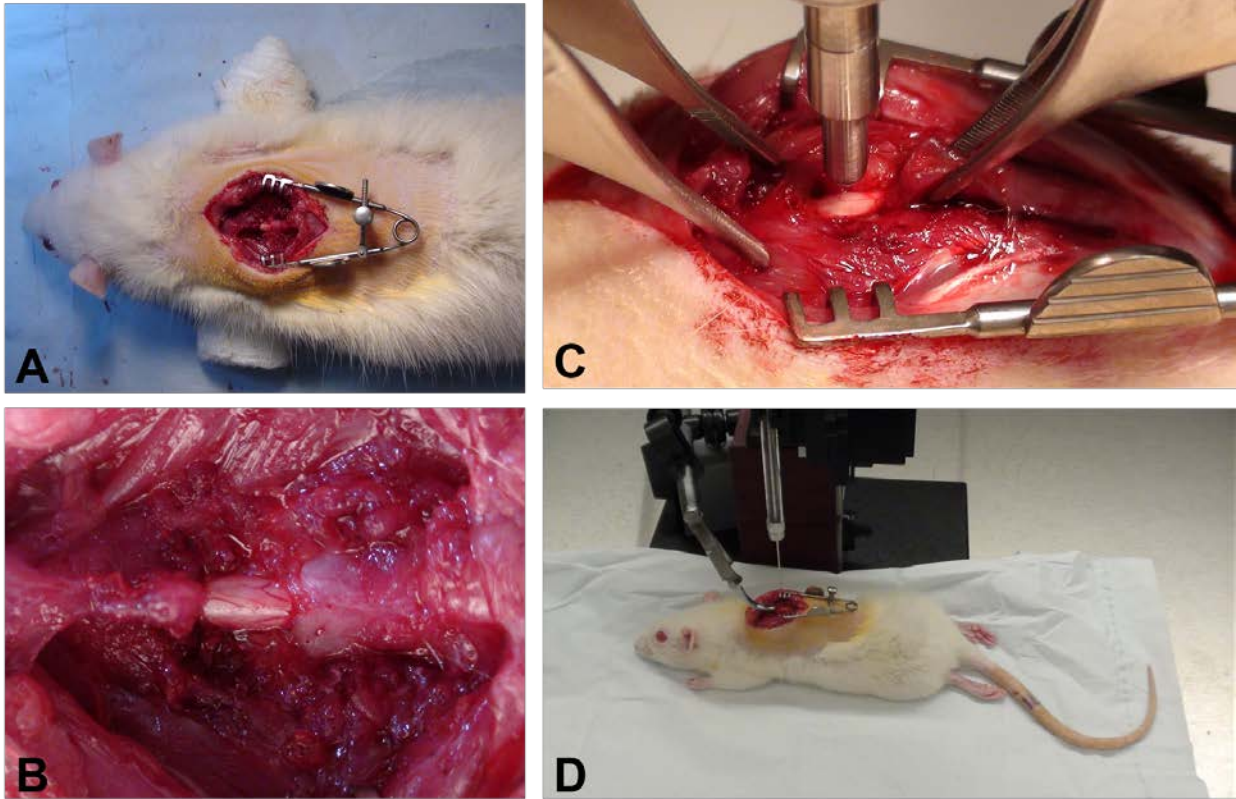
Figure 20 Spinal cord injury and injection. A) Laminectomy was performed at thoracic level and B) T9 spinal segment was exposed. C) Contusion injury with Infinite Horizon impactor. D) Injection apparatus for 3dpi injection of aLam, nLam or PBS.

3.2.2.2 Post-Surgery Procedures

Antisedan (1.5 mg/kg; Pfizer) was injected subcutaneously to reverse the effects of dexdomitor. An intramuscular injection of gentamicin (6 mg/kg; VWR) and subcutaneous injections of Rimadyl (5 mg/kg; Pfizer) and Ringer's solution (10 mL on the surgery day, 5 mL thereafter) were administered daily for three days post injury. After injection on the third day after injury,

rats received daily injections with gentamicin for four days Rimadyl and Ringer's for three days. Bladders were expressed manually twice daily until reflex voiding returned. A ll rats were monitored daily throughout the course of experiment and exhibited no sign of additional stress or pain response. R ats were perfusion fixed with 1 x PBS followed by 4 % Paraformaldehyde (PFA) at seven weeks post injury.

3.2.2.3 Motor Function Assessment

All motor function assessments were conducted by one or more investigators (depending on the tested motor task) blinded to the treatment group. O verground walking ability was assessed using the BBB test (70) (Figure 21) one and three days post injury and weekly thereafter (n=10/group). Individual scores were averaged across paws and used for experimental group averages. Sensorimotor function was assessed using the horizontal ladder walking tests (aLam (n=10); nLam (n=7); PBS (n=9)) at three and six weeks post injury (Figure 21). Medium (foot and partial leg) and large (full leg) slips were counted and expressed as a percentage of the total number of steps. Percent scores were averaged across experimental group. Gait at a w alking speed of 20 cm/sec was assessed using the DigiGait^{TM} Image Analysis system (Figure 12) at one day prior to (baseline) (n=10/group) and six weeks post injury (aLam (n=7); nLam (n=9); PBS (n=9)). H ind limb stride length was expressed as a p ercent of the baseline value and averaged between paws and within groups.
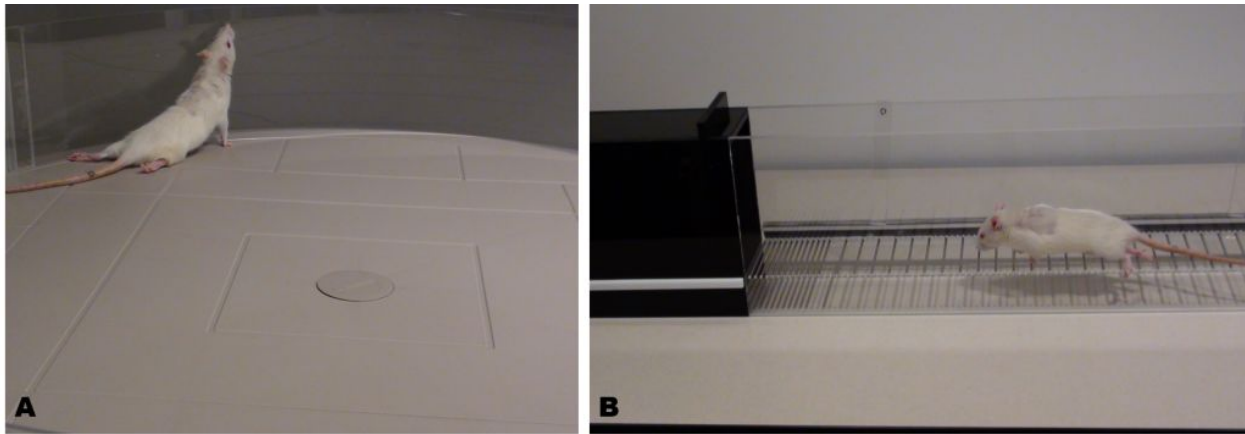
Figure 21 BBB and Horizontal Ladder. A) Image of spinal cord injured rat completing BBB evaluation of overground walking. B) Image of spinal cord injured rat transversing horizontal ladder sensorimotor task.

3.2.2.4 Sensory Function Assessment

All sensory function assessments were conducted by one or more investigators blinded to treatment group of rats. Mechanical alloydynia was assessed using Von Frey hairs, previously shown to detect changes in sensitivity using this injury model (68). Animals were placed in Plexiglas boxes on a raised grid platform and allowed to acclimate until visibly relaxed and still. Rigid filaments were applied to the plantar surface of each hindpaw at increasing force (g) until withdrawal. To reduce variability, test was repeated five times per paw at 5 min intervals and the middle three scores were recorded and averaged per time point. Testing was conducted at one day prior to (baseline) and three and six weeks post injury (n=10/group). Scores were expressed as a percentage of the baseline score and averaged across paws and within groups.

Thermal hypersensitivity was measured using the Hargreaves assay (72). Rats were placed in Plexiglas boxes on a raised glass platform and allowed to acclimate until visibly relaxed and still. A high-intensity beam of light was focused on the plantar surface of each

hindpaw and seconds to withdrawal was measured. The active beam intensity was set at 25 %, resting intensity at 5 %, and cutoff at 20 sec to ensure no tissue damage was done. To reduce variability, test was repeated five times per paw at 5 min intervals and the middle three scores were recorded and averaged per time point. Testing was conducted at one day prior to (baseline) and three and six weeks post injury (n=10/group). Scores are expressed as a percentage of the baseline score and averaged across paws and within groups.

3.2.2.5 Anterograde and Retrograde Tracing

Biotinylated Dextran Amine (10 % BDA, 10,000 MW; Molecular Probes, #D1956, Lot: 1476602) was inject bilaterally into the motor cortex six weeks post injury. The skull was exposed and two small diameter holes were drilled directly above the motor cortex. Three μL of 1 % BDA was injected per hemisphere to anterogradely trace the corticospinal axons. Traced axons were visualized using TSA Cyanide-3 Amplification Kit (PerkinElmer, NEL704A1001KT). Labeled axons 1 mm above and below the lesion cavity were counted, multiplied by ten (one out of ten sections were used for quantification) and expressed as percent regenerated/spared ((below/above)*100). Totals were averaged per experimental group.

Retrograde tracing was performed using 2 % Fast Blue (0.6μL each spinal hemisphere; Sigma, #F337813), injected 10 mm caudal to injury. Brainstem sections were cut into ten series using the cryostat microtome (40 μm, -24 ºC, free-floating). One series was mounted on positively charged slides and the total number of labeled neurons in the red nuclei was counted using a Zeiss Plan Apochromat objective (20x air, NA 0.8). The numbers were multiplied by ten and averaged per group.

3.2.2.6 Histology

Ten days after injection of tracer, animals were deeply anesthetized (100 mg/kg Ketamine) and transcardially perfused with 300 mL of 0.01 M PBS followed by 400 mL of 4 % paraformaldehyde (PFA). Spinal cords were then dissected and post-fixed overnight at 4 ºC in 4 % PFA then transferred into a cryoprotective 30 % sucrose solution and stored at 4 ºC. A 15 mm-long piece of the spinal cord centered on the injury site was dissected from spinal cord cut into 10 series of 15 µm-thick horizontal sections on a cryostat microtome and mounted on positively charged microscope slides. One series was used for Nissl staining for spared tissue quantification. All other series were used for immunohistochemistry.

3.2.2.7 Immunohistochemistry

Nonspecific binding sites were blocked using 0.01M PBS with 5 % Normal Goat Serum (NGS) and 0.03 % Triton blocking solution at room temperature for 30 min. Tissue was then incubated with primary antibodies against astrocytes (GFAP; DAKO, 1:200) and neurofilament-h (RT-97; Millipore, 1:200) diluted in blocking solution for 2 h at room temperature or overnight in 4 ºC. Fluorescent secondary antibodies diluted in 0.01 M PBS (Alexa Fluor®, life technologies, 1:500) were added for 1 h at room temperature, followed by DAPI counterstaining and covered with glass slips with anti-fade fluorescent mounting media (Dako, #S3023, Carpenteria, CA USA). Tissue was evaluated using a Zeiss Axio Observer inverted fluorescent microscope with Zeiss Plan Apochromat objective (20x air, NA 0.8), and StereoInvestigator® (MBF Biosciences, Inc.) software.

3.2.2.8 Spared Tissue Quantification

Nissl stained sections were used to determine the volume of spared tissue within the area of injury using a Zeiss Axio Observer inverted microscope and the Cavalieri estimator function of StereoInvestigator software (MicroBrightField, Inc). Analysis was performed by an investigator blinded to experimental condition. The spared tissue areas of all sections were used to calculate the volume of spared tissue in the series and multiplied by 10 to represent tissue across the entire cord segment, totals were averaged per experimental group (n=10/group).

3.2.2.9 Statistical Analysis

Factorial ANOVA with Tukey's post hoc was used to analyze histological and tracing differences between groups. R epeated measures mixed ANOVA with Tukey's post hoc was used to evaluated differences in behavioral measures. Significance was set at $p \leq 0.05$.

3.2.3   Results

3.2.3.1 Laminin did not affect motor function recovery

Multiple tests were conducted to comprehensively evaluate motor function in the injured and treated rats. Laminin polymer treatment did not affect overground walking as measured by the BBB or sensorimotor function as measured by the horizontal ladder test (Figure 22). Differences in gait were assessed using the DigiGait and no effect of group was found in stride length and paw rotation, outcome measures that normally are associated with SCI (Figure 23).
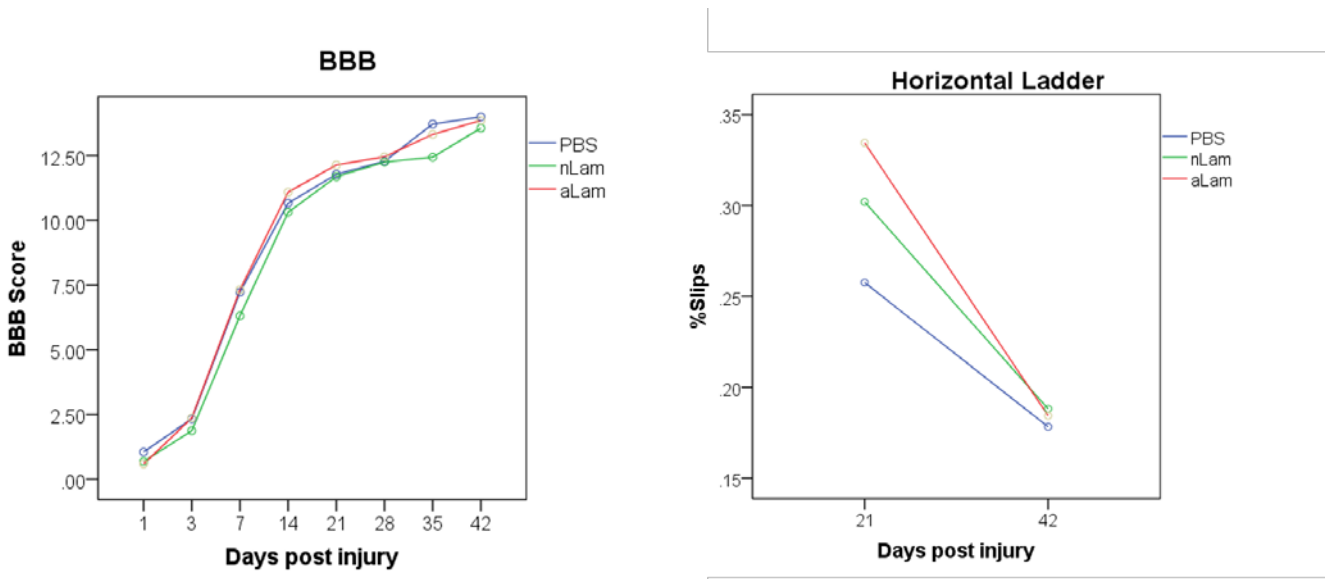
Figure 22 BBB and Horizontal ladder. Polymerized laminin did not affect recovery of overground walking (BBB; p=0.4) or sensorimotor integration (horizontal ladder; p=0.7)
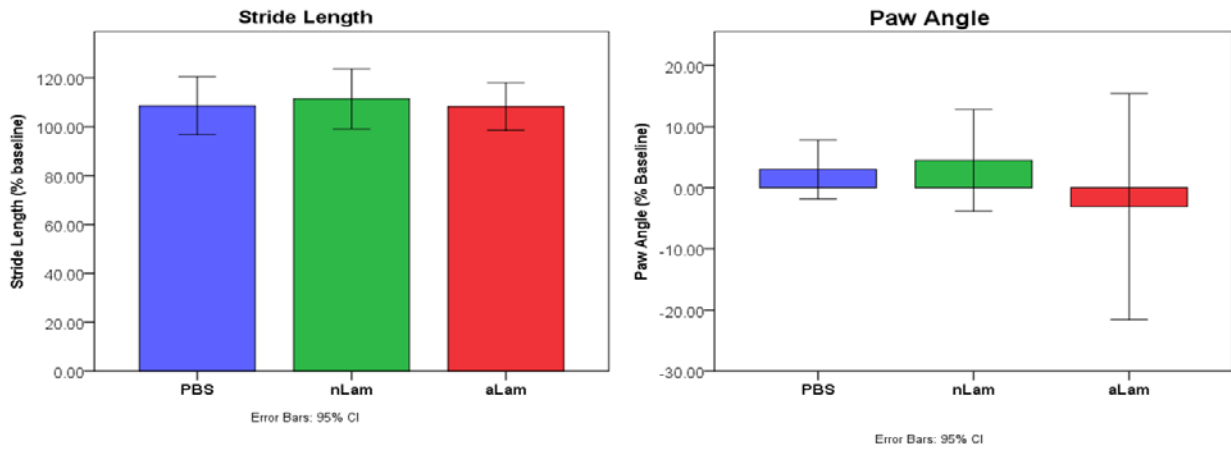
Figure 23 Gait Analysis. Polymerized laminin injection did not affect gait recovery measurements at 6 weeks post injury (MANOVA, Stride length; p=0.68, Paw angle; p=0.49)

3.2.3.2 Laminin did not affect sensory function recovery

In order to evaluate sensory function, the Hargreaves test was used to assess thermal hyperalgesia and the Von Frey test for mechanical allodynia. We found that none of the injured and treated animals developed allodynia (data not shown). All rats exhibited symptoms of thermal hyperalgesia. The control group and the nLam-treated group had higher sensitivity for the thermal stimulus than the aLam-treated group, but the group differences did not reach statistical significance (p=0.5) (Figure 24).
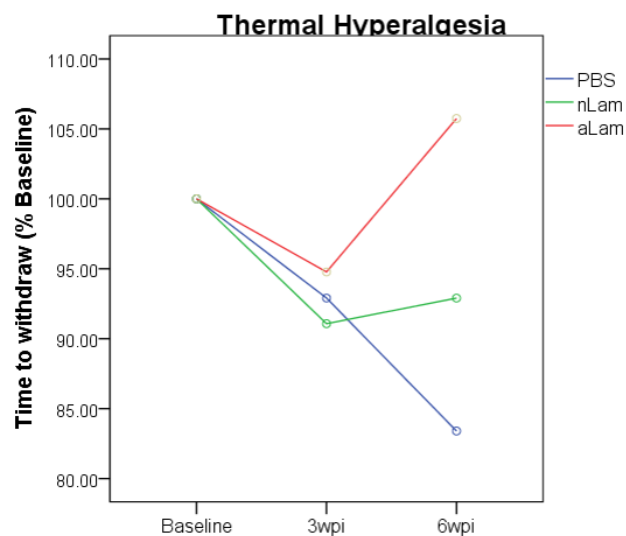
Figure 24-Thermal Hyperalgesia. Thermal hyperalgesia was measured using the Hargreaves method (resting intensity 5%, active intensity 25%, 20sec max). No main effect of group was observed using repeated measures ANOVA (p=0.5).

3.2.3.3 Laminin polymers decrease astrocyte activation

Astrocyte activation was measured using antibodies against glial-fibrillary acidic protein (GFAP). Laminin polymer treatment resulted in a significant effect of group (p=0.008) showing

significant decreases in staining intensity of GFAP relative to the PBS group (PBS vs aLam or nLam, $p<0.05$) (Figure 25). No difference in the effects of aLam and nLam on astrocyte activity was detected ($p=0.85$).

3.2.3.4 aLam did not affect axon intensity at injury site

Axons were identified using antibodies against neurofilament-h and the staining intensity measured. We found a significant effect of group ($p=0.01$). Tukey's post hoc revealed aLam treatment did not affect axon intensity relative to PBS group. nLam treatment, however, showed significantly decreased axon intensity across the injury site relative to PBS (Figure 25, $p<0.01$).
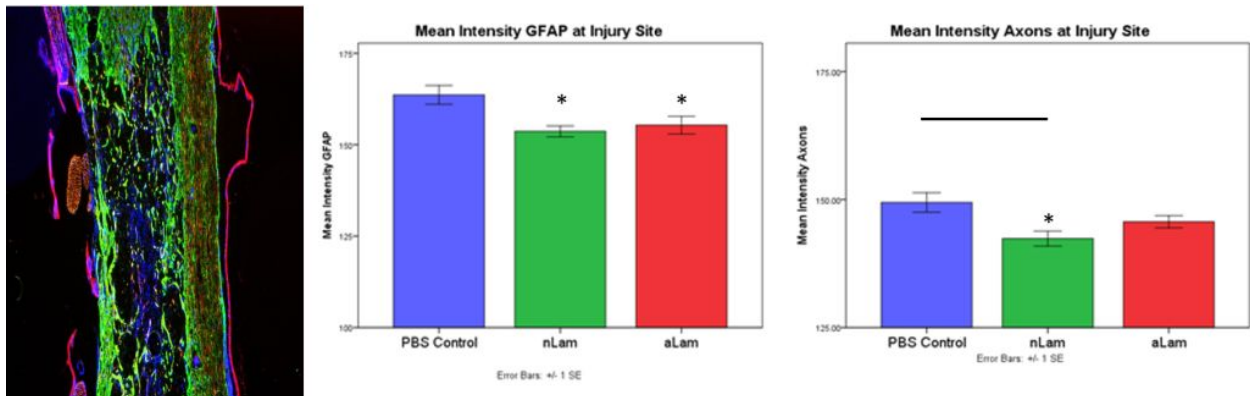
Figure 25 Astrocyte Activation and Axons. Significant decrease in GFAP intensity at the injury site in laminin treatment groups ($p<0.05$). Significant decrease in axon intensity at injury site in nLam group vs PBS ($p<0.01$), no difference between PBS and aLam group. Image: GFAP (green), RT97 (neurofilament, red), DAPI (blue).

3.2.3.5 Anterograde and Retrograde tracing

Fast Blue (FB) retrograde tracing and BDA anterograde tracing were used to determine number of axons originating from the red nuclei or primary motor cortex, respectively. There was no effect of group on either population of axons (Figure 26).
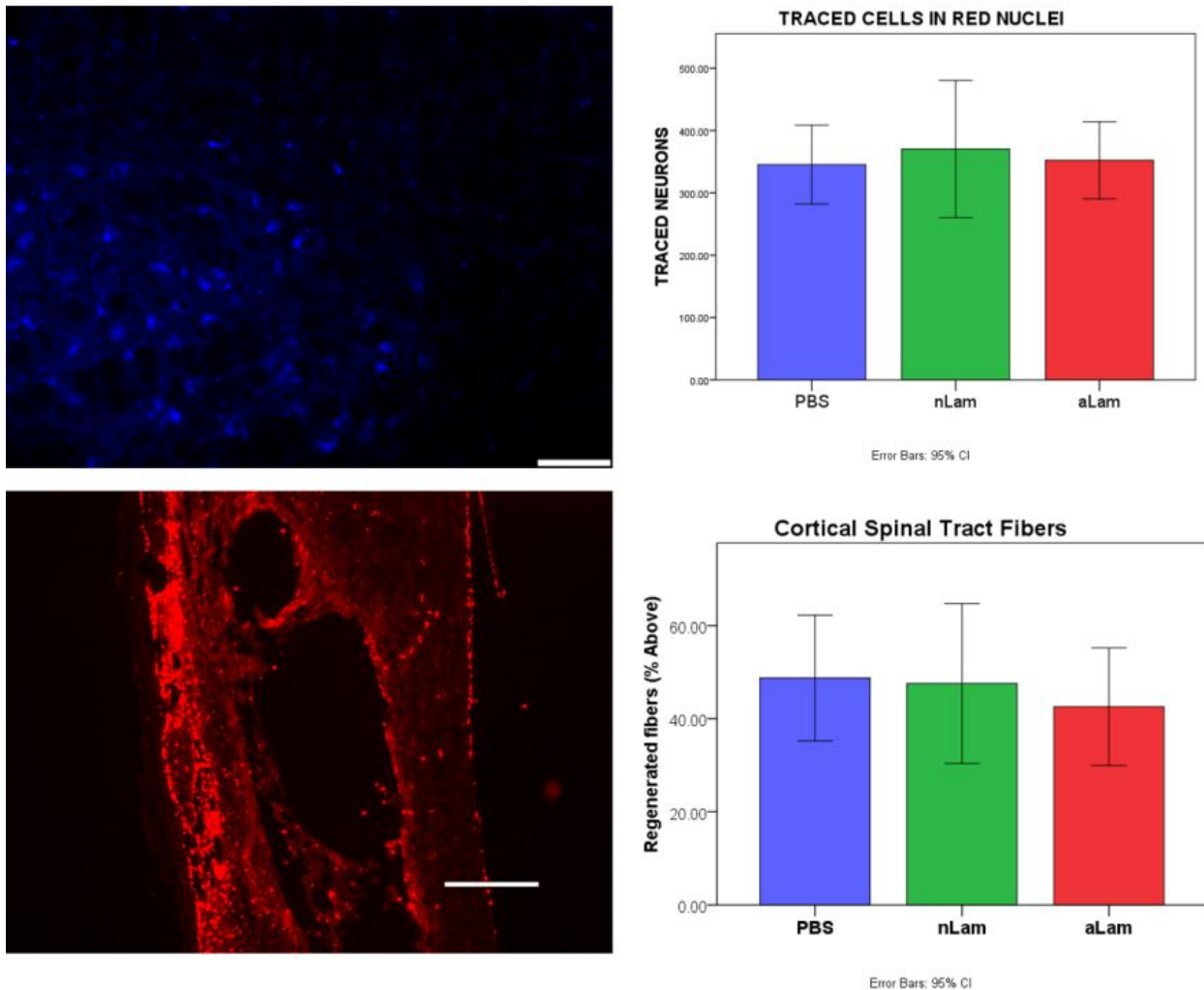
Figure 26 Tracing Quantification. A) Fast blue traced neurons in the red nucleus (Scale bar=100µm). No difference between groups was observed (ANOVA, p=.8). B) BDA traced axons at the injury site (Scale bar=100µm). Graph expresses count 1mm below injury as a percentage of 1mm above injury cavity. No effect of group (ANOVA, p=.77).

3.2.3.6 Polymerized laminin had no effect on tissue sparing

Nissl staining was used to enable identification of lost tissue and analysis of spared tissue in the contused segment. Injection of laminin polymers did not affect the volume of spared tissue (p=0.2) (Figure 27).
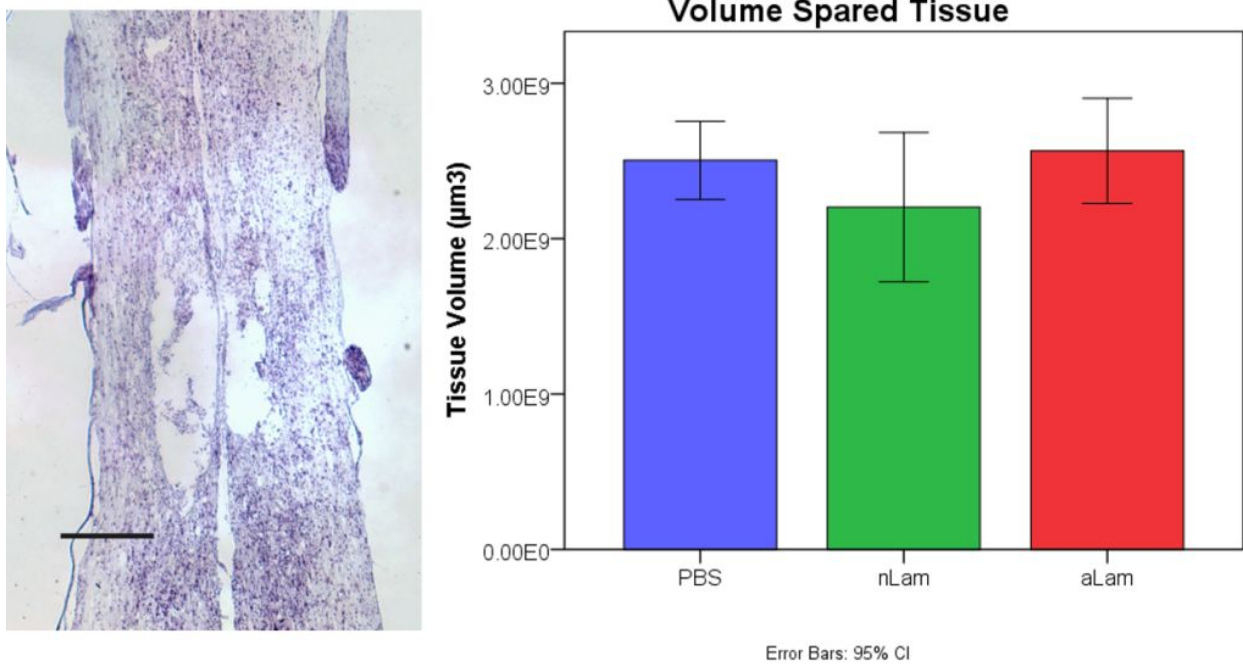
Figure 27 Tissue Sparing. Nissl staining of spinal segments were quantified for total volume (Scale bar= 100μm). Graph represents group means with 95% confidence interval. No effect of group (ANOVA, p=.26)

3.2.4 Discussion

Our results from the study described in Chapter 3.1, suggested that aLam elicits axonal growth responses in an injured peripheral nerve. H ere, we have evaluated whether aLam promotes axonal responses in the contused adult rat spinal cord. Our findings suggest that 1) laminin polymers do not affect the total number of axons in general, and corticospinal or rubrospinal tract fibers specifically at the injury site; 2) laminin polymers do not affect motor or sensory recovery at six weeks following an injury; 3) laminin polymer presence decreases astrocyte activation; 5) laminin polymer injections do not affect spared tissue volume. In summary, aLam reduced astrocytic activation in the contused spinal cord segment, but this did not result in enhanced axon regeneration and functional recovery.

The lack of effects on axon responses by aLam may suggests that the timing of the treatment or the concentration/amount of the injected laminin polymer was suboptimal for eliciting an effect. SCI presents an environment full of inhibitory molecules and high levels of inflammation. It is a daunting task to overcome the many growth-inhibitory factors in order to elicit regeneration. A mong the inhibition encountered at the lesion site is reactive astrocytes composing the glial scar. This 'scar' form a physical and chemical barrier to growth surrounding the injury. An immediate injection may better utilize aLam's effect on astrocyte activation and could be more suitable for decreasing inhibition in order to observe optimal benefits from its growth-promoting abilities. Another consideration is the site of injection. O ur integrin immunostaining before and after injury indicated an increased expression on m otor neurons above and below the epicenter, perhaps multiple injections in those locations would prove more favorable than a single injection into the epicenter. Future research will be necessary to elucidate the validity of these possible explanations.

4.0 SUMMARY AND GENERAL DISCUSSION

Together the results obtained from the experiments described in this thesis provide a thorough evaluation of the *in vitro* and *in vivo* potential of laminin polymerized under acidic pH conditions for neurite extension and axon regeneration. In the first part of our *in vitro* work using a novel developed model system (Chapter 2.1), our results provided information about the integrin receptor targets of aLam to enhance neurite growth competence of adult neurons and that aLam elicits compensatory measures to up regulate $\alpha 3$ integrins in the 'absence' of availability of $\alpha 1$ integrins. The data also showed that aLam enhances neurite outgrowth by increasing focal adhesion complex formation, which is necessary for actin polymerization and axon extension. That aLam elicits its response through multiple growth-promoting binding sites and can initiate a compensatory response in the absence of one is an important characteristic because it increases the overall impact of aLam as a treatment for nervous tissue repair. Integrin expression is a dynamic process following injury, as is evidenced from the significant increase in expression of $\alpha 1$ and $\alpha 3$ at three days after SCI. As the injury environment changes with time, it has been shown that integrin expression changes as well (73). Detailed information on longitudinal integrin expression profiles in response to a specific injury mechanism is needed to fully realize the potential therapeutic window of aLam.

In second part of our *in vitro* work (Chapter 2.2), we showed that microcontact printing is an appropriate way to observe directed growth of neurons cultured on growth-neutral PDL

substrates and that when translated to the live imaging environment, attached neurons are able to remain viable in this system for long periods of time, regardless if they were imaged using the Bioptechs chamber or culture dishes. This is an important proof of concept to take into consideration in the design of future live imaging experiments. This finding suggests that our PDL concentration, media components, and choices of imaging modality and duration are all appropriate for these types of neurons. Optimizing this system to retain greater cell adhesion and growth in order to be able to evaluate dynamic interactions is an important next step.

In the *in vivo* experiments (Chapter three) we found that aLam injected into a damaged peripheral nerve, resulted in an axonal regeneration response. In addition, aLam treatment decreased autophagia and increased treadmill task compliance. Our spinal cord data revealed that the effect of aLam is not exclusive to neurons, which was apparent through the decrease in activated astrocytes at the injury site. However, since this action did not result in enhanced growth in our model system, it is impossible to definitively determine from the present results whether it is related to regeneration, or an unrelated, potentially beneficial side effect.

Our first goal of this thesis was to utilize a novel *in vitro* system to test the molecular and cellular mechanisms of aLam as a growth-promoting molecule. In Chapter 2.1 we successfully tested our novel *in vitro* system and our results revealed that aLam maintains its growth-promoting effects through binding of the α1 and α3 integrin receptors and increasing focal adhesion complex formation. Our second goal was to employ microcontact printing and live imaging to create a system in which to study aLam's effect on growth cone dynamics and glial cell involvement. Early results from this support the feasibility of utilizing this technique in that we were able to achieve directed growth on PDL stamped substrates in culture and cells retained viability for the duration of the live imaging. Together these suggests that with optimization of

pattern and technique, microcontact printing of PDL and live imaging would be an appropriate and valuable combination tool for use in the assessment of neural growth dynamics with unbound signaling molecules. Our third goal was to test the repair potential of aLam as an injectable regenerative therapeutic using an adult rat model of PNI. This was accomplished using a clinically relevant model of rat peroneal crush injury. Results showed that aLam elicited therapeutic effects on axon growth, task compliance and autophagia. Axon growth effects did not lead to improvements in motor function. Results on autophagia are novel and clinically relevant and future studies should be conducted to better understand this phenomenon. Our fourth goal was to test the repair potential of aLam as an injectable regenerative therapeutic using an adult rat model of SCI. This was accomplished using a clinically relevant model of contusion SCI. Results showed that aLam did not elicit axon regeneration or functional recovery. There was a novel and clinically relevant aLam-mediated decrease in activated glia at and surrounding the contusion.

Taken together we have shown here that organization of polymerized laminin can have significant impact on how it interacts with receptors and promotes signaling for growth and that this signaling is not substrate attachment dependent, but rather acts as an unbound environmental signaling ligand. This increases the potential impact for treatment development in that it retains the potential for use in delicate tissues and 'closed systems' where injectable treatments are preferable because they cause minimal addition damage to nervous tissue. Our results here indicate that the differences found between aLam and nLam could be due to their structure. Further work is needed to definitively determine if structural differences are underlying changes observed in receptor interaction and growth-promotion. Elucidating meaningful differences in three dimensional structure of this polymer could impact the development of novel biomaterials

as well as future consideration in the use of ECM proteins for signaling and repair. Our goals stated above have been accomplished through new, innovative approaches accompanying time-tested established models. The marriage of these allowed for us to reveal novel and interesting results that could potentially change the way people think about and test extracellular matrix molecules for injectable therapeutics.

Although aLam did not, in our model, promote axon regeneration that led to functional repair *in vivo*, the combined studies provided important groundwork for engineering new, more efficient molecular structures for specific targeting of multiple integrin receptors for neural regeneration.

BIBLIOGRAPHY

1.   Barroso M, Freire E, Limaverde G, Rocha G, Batista E, Weissmuller G, et al. Artificial Laminin Polymers Assembled in Acidic pH Mimic Basement Membrane Organization. Journal of Biological Chemistry. 2008;283(17):11714-20.

2.   Freire E, Gomes F, Linden R, Neto V, Coelho-Sampaio T. Structure of laminin substrates modulates cellular signaling for neuritogenesis. Journal of Cell Science. 2002;115:4867-76.

3.   Association TN. The Neuropathy Association: The Neuropathy Association; 2014 [cited 2014 october 19, 2014]. Available from: http://www.neuropathy.org/site/News2?page=NewsArticle&id=8445&news_iv_ctrl=1101.

4.   Grzywacz JG, McMahan S, Hurley JR, Stokols D, Phillips K. Serving racial and ethnic populations with health promotion. American journal of health promotion : AJHP. 2004;18(5):suppl 8-12. PubMed PMID: 15163143.

5.   Pfister BJ, Gordon T, Loverde JR, Kochar AS, Mackinnon SE, Cullen DK. Biomedical engineering strategies for peripheral nerve repair: surgical applications, state of the art, and future challenges. Critical reviews in biomedical engineering. 2011;39(2):81-124. PubMed PMID: 21488817.

6.   Rauck BM, Novosat TL, Oudega M, Wang Y. Biocompatibility of a coacervate-based controlled release system for protein delivery to the injured spinal cord. Acta biomaterialia. 2014. doi: 10.1016/j.actbio.2014.09.037. PubMed PMID: 25266504.

7.   Ritfeld GJ, Rauck BM, Novosat TL, Park D, Patel P, Roos RA, et al. The effect of a polyurethane-based reverse thermal gel on bone marrow stromal cell transplant survival and spinal cord repair. Biomaterials. 2014;35(6):1924-31. doi: 10.1016/j.biomaterials.2013.11.062. PubMed PMID: 24331711; PubMed Central PMCID: PMC3906670.

8.   Chen YS, Hsieh CL, Tsai CC, Chen TH, Cheng WC, Hu CL, et al. Peripheral nerve regeneration using silicone rubber chambers filled with collagen, laminin and fibronectin. Biomaterials. 2000;21(15):1541-7. PubMed PMID: 10885726.

9.   Cao J, Xiao Z, Jin W, Chen B, Meng D, Ding W, et al. Induction of rat facial nerve regeneration by functional collagen scaffolds. Biomaterials. 2013;34(4):1302-10. doi: 10.1016/j.biomaterials.2012.10.031. PubMed PMID: 23122676.

10.   Council AC. The Basics: Polymer Definition and Properties http://plastics.americanchemistry.com/The-Basics: American Chemistry Council, Inc; 2005-2013 [cited 2013 F ebruary 25, 2013] . Available from: http://plastics.americanchemistry.com/The-Basics.

11.   Ratner BD, Lemons J, Schoen F, Hoffman AS. Biomaterials Science: An Introduction to Materials in Medicine. Second ed. San Diego: Academic Press; 2004 A ugust 1st 2004. 864 p.

12.   Williams DF. On the mechanisms of biocompatibility. Biomaterials. 2008;29(20):2941-53. doi: 10.1016/j.biomaterials.2008.04.023. PubMed PMID: 18440630.

13.   Sanes JR. Extracellular matrix molecules that influence neural development. Annu Rev Neurosci. 1989;12:491-516. doi: 10.1146/annurev.ne.12.030189.002423. PubMed PMID: 2648958.

14.   Reichardt LF, Tomaselli KJ. Extracellular matrix molecules and their receptors: functions in neural development. Annu Rev Neurosci. 1991;14:531-70. doi: 10.1146/annurev.ne.14.030191.002531. PubMed PMID: 1851608; PubMed Central PMCID: PMC2758225.

15.   Calof AL, Lander AD. Relationship between neuronal migration and cell-substratum adhesion: laminin and merosin promote olfactory neuronal migration but are anti-adhesive. The Journal of cell biology. 1991;115(3):779-94. PubMed PMID: 1918163; PubMed Central PMCID: PMC2289183.

16.   Busch SA, Silver J. The role of extracellular matrix in CNS regeneration. Curr Opin Neurobiol. 2007;17(1):120-7. doi: 10.1016/j.conb.2006.09.004. PubMed PMID: 17223033.

17.   Tomaselli KJ. Beta 1-integrin-mediated neuronal responses to extracellular matrix proteins. Annals of the New York Academy of Sciences. 1991;633:100-4. PubMed PMID: 1724124.

18.   Ruoslahti E. RGD and other recognition sequences for integrins. Annu Rev Cell Dev Biol. 1996;12:697-715. doi: 10.1146/annurev.cellbio.12.1.697. PubMed PMID: 8970741.

19.   Liu J, Chen J, Liu B, Yang C, Xie D, Zheng X, et al. Acellular spinal cord scaffold seeded with mesenchymal stem cells promotes long-distance axon regeneration and functional recovery in spinal cord injured rats. J Neurol Sci. 2013;325(1-2):127-36. doi: 10.1016/j.jns.2012.11.022. PubMed PMID: 23317924.

20. Medberry CJ, Crapo PM, Siu BF, Carruthers CA, Wolf MT, Nagarkar SP, et al. Hydrogels derived from central nervous system extracellular matrix. Biomaterials. 2013;34(4):1033-40. doi: 10.1016/j.biomaterials.2012.10.062. PubMed PMID: 23158935; PubMed Central PMCID: PMC3512573.

21. Azemi E, Lagenaur CF, Cui XT. The surface immobilization of the neural adhesion molecule L1 on ne ural probes and its effect on ne uronal density and gliosis at the probe/tissue interface. Biomaterials. 2011;32(3):681-92. doi: 10.1016/j.biomaterials.2010.09.033. PubMed PMID: 20933270; PubMed Central PMCID: PMC3394228.

22. Badylak SF. The extracellular matrix as a scaffold for tissue reconstruction. Semin Cell Dev Biol. 2002;13(5):377-83. PubMed PMID: 12324220.

23. Colognato H, Winkelmann D, Yurchenco P. Laminin polymerization induces a receptor-cytoskeleton network. Journal of Cell Biology. 1999;145(3):619-31.

24. Tomaselli K, Hall D, Flier L, Gehlsen K, Turner D, Carbonetto S, et al. A neuronal cell line (PC12) expresses two β_1 class integrins $\alpha_1\beta_1$ and $\alpha_3\beta_1$-that recognize different neurite outgrowth-promoting domains in laminin. Neuron. 1990;5:651-62.

25. Cornbrooks CJ, Carey DJ, McDonald JA, Timpl R, Bunge RP. In vivo and in vitro observations on l aminin production by Schwann cells. Proceedings of the National Academy of Sciences of the United States of America. 1983;80(12):3850-4. Epub 1983/06/01. PubMed PMID: 6344090; PubMed Central PMCID: PMC394150.

26. Plantman S, Patarroyo M, Fried K, Domogatskaya A, Tryggvason K, Hammarberg H, et al. Integrin-laminin interactions controlling neurite outgrowth from adult DRG neurons *in vitro*. Molecular and Cellular Neuroscience. 2008;39(1):50-62.

27. Liesi P. Do neurons in the vertebrate CNS migrate on l aminin? EMBO Journal. 1985;4(5):1163-70.

28. Liesi P. Laminin-immoreactive glia distinguish regenerative adult CNS systems from non-regenerative ones. EMBO Journal. 1985;4(10):2505-11.

29. Tate C, Shear D, Tate M, Archer D, Stein D, LaPlaca M. Laminin and fibronectin scaffolds enhance neural stem cell transplantation into the injured brain. Journal of Tissue Engineering and Regenerative Medicine. 2009;3:208-17.

30. Menezes K, Lacerda de Menezes J, Nascimento M, de Siqueira Santos R, Coelho-Sampaio T. Polylaminin, a polymeric form of laminin, promotes regeneration after spinal cord injury. FASEB. 2010;24(4513-4522).

31. Verdu E, Labrador RO, Rodriguez FJ, Ceballos D, Fores J, Navarro X. Alignment of collagen and laminin-containing gels improve nerve regeneration within silicone tubes.

Restor Neurol Neurosci. 2002;20(5):169-79. Epub 2003/01/08. PubMed PMID: 12515893.

32.   Kleinman HK, Martin GR. Matrigel: basement membrane matrix with biological activity. Semin Cancer Biol. 2005;15(5):378-86. doi: 10.1016/j.semcancer.2005.05.004. PubMed PMID: 15975825.

33.   Tsai EC, Dalton PD, Shoichet MS, Tator CH. Matrix inclusion within synthetic hydrogel guidance channels improves specific supraspinal and local axonal regeneration after complete spinal cord transection. Biomaterials. 2006;27(3):519-33. doi: 10.1016/j.biomaterials.2005.07.025. PubMed PMID: 16099035.

34.   Labrador RO, Buti M, Navarro X. Influence of collagen and laminin gels concentration on nerve regeneration after resection and tube repair. Experimental neurology. 1998;149(1):243-52. doi: 10.1006/exnr.1997.6650. PubMed PMID: 9454634.

35.   Tate MC, Garcia AJ, Keselowsky BG, Schumm MA, Archer DR, LaPlaca MC. Specific beta1 integrins mediate adhesion, migration, and differentiation of neural progenitors derived from the embryonic striatum. Molecular and cellular neurosciences. 2004;27(1):22-31. doi: 10.1016/j.mcn.2004.05.001. PubMed PMID: 15345240.

36.   Colognato H, Yurchenco P. Form and Function: The Laminin Family of Heterotrimers. Developmental Dynamics. 2000;218:213-34.

37.   Mruthyunjaya S, Manchanda R, Godbole R, Pujari R, Shiras A, Shastry P. Laminin-1 induces neurite outgrowth in human mesenchymal stem cells in serum/differentiation factors-free conditions through activation of FAK-MEK/ERK signaling pathways. Biochemical and biophysical research communications. 2010;391(1):43-8. doi: 10.1016/j.bbrc.2009.10.158. PubMed PMID: 19895795.

38.   Bozyczko D, Horwitz A. The participation of putative cell surface receptor for laminin and fibronectin in peripheral neurite extension. J Neurosci. 1986;6(1241-1251).

39.   Liesi P, Laatikainen T, Wright J. A biologically active sequence (KDI) mediates the neurite outgrowth function of the gamma1 chain of laminin-1. Journal of neuroscience research. 2001;66:1046-52.

40.   Conklin MW, Lin MS, Spitzer NC. Local calcium transients contribute to disappearance of pFAK, focal complex removal and deadhesion of neuronal growth cones and fibroblasts. Dev Biol. 2005;287(1):201-12. Epub 2005/10/06. doi: S0012-1606(05)00600-7 [pii] 10.1016/j.ydbio.2005.09.006. PubMed PMID: 16202989.

41.   Renaudin A, Lehmann M, Girault J, McKerracher L. Organization of point contacts in neuronal growth cones. Journal of neuroscience research. 1999;55(4):458-71. PubMed PMID: 10723056.

42. Palecek S, Loftus J, Ginsberg M, Lauffenburger D, Horwitz A. Itegrin-ligand binding properties govern cell migration speed through cell-substratum adhesiveness. Nature. 1997;385:537-40.

43. Kumar A, Whitesides GM. Features of gold having micrometer to centimeter dimensions can be formed through a combination of stamping with an elastomeric stamp and an alkanethiol "ink" followed by chemical etching. Appl Phys Lett. 1993;63(2002). doi: http://dx.doi.org/10.1063/1.110628.

44. Palchesko RN, Zhang L, Sun Y, Feinberg AW. Development of polydimethylsiloxane substrates with tunable elastic modulus to study cell mechanobiology in muscle and nerve. PloS one. 2012;7(12):e51499. doi: 10.1371/journal.pone.0051499. PubMed PMID: 23240031; PubMed Central PMCID: PMC3519875.

45. Bernard A, Renault JP, Michel B, Bosshard HR, Delamarche E. Microcontact Printing of Proteins. Advanced Materials. 2000;12(14).

46. James CD, Davis R, Meyer M, Turner A, Turner S, Withers G, et al. Aligned microcontact printing of micrometer-scale poly-L-lysine structures for controlled growth of cultured neurons on planar microelectrode arrays. IEEE transactions on bio-medical engineering. 2000;47(1):17-21. PubMed PMID: 10646274.

47. Thiebaud P, Lauer L, Knoll W, Offenhausser A. PDMS device for patterned application of microfluids to neuronal cells arranged by microcontact printing. Biosensors & bioelectronics. 2002;17(1-2):87-93. PubMed PMID: 11742739.

48. Wheeler BC, Corey JM, Brewer GJ, Branch DW. Microcontact printing for precise control of nerve cell growth in culture. Journal of biomechanical engineering. 1999;121(1):73-8. PubMed PMID: 10080092.

49. Seddon H. Surgical disorders of the peripheral nerves. 2d ed. Edinburgh ; New York: Churchill Livingstone; 1975. xiii, 336 p. p.

50. Sunderland S. Nerves and nerve injuries. 2d ed. Edinburgh ; New York, New York: Churchill Livingstone ; distributed by Longman; 1978. xii, 1046 p. p.

51. Haymaker W, Woodhall B. Peripheral nerve injuries; principles of diagnosis. 2d ed. Philadelphia,: Saunders; 1953. xv, 333 p. p.

52. Robinson LR. Traumatic injury to peripheral nerves. Muscle & nerve. 2000;23(6):863-73. PubMed PMID: 10842261.

53. Seddon HJ. Nerve Grafting. The Journal of bone and joint surgery British volume. 1963;45:447-61. PubMed PMID: 14058318.

54. One Degree of Separation: Paralysis and Spinal Cord Injury in the United States. Christopher and Dana Reeve Foundation, 2010.

55.   The University of Alabama National Spinal Cord Injury Statistical Center, Centers for Disease Control and Prevention, 2010.

56.   Giancotti FG, Ruoslahti E. Integrin signaling. Science. 1999;285(5430):1028-32. PubMed PMID: 10446041.

57.   Malin S, Davis B, Molliver D. Production of dissociated sensory neuron cultures and consideration for their use in studying neuronal function and plasticity. Nature Protocols. 2007;2(1):152-60.

58.   Schneider CA, Rasband WS, Eliceiri KW. NIH Image to ImageJ: 25 years of image analysis. Nat Methods. 2012;9(7):671-5. PubMed PMID: 22930834.

59.   Miyamoto S, Katz BZ, Lafrenie RM, Yamada KM. Fibronectin and integrins in cell adhesion, signaling, and morphogenesis. Annals of the New York Academy of Sciences. 1998;857:119-29. Epub 1999/01/26. PubMed PMID: 9917837.

60.   Chang JC, Brewer GJ, Wheeler BC. A modified microstamping technique enhances polylysine transfer and neuronal cell patterning. Biomaterials. 2003;24(17):2863-70. PubMed PMID: 12742724.

61.   Viader A, Chang LW, Fahrner T, Nagarajan R, Milbrandt J. MicroRNAs modulate Schwann cell response to nerve injury by reinforcing transcriptional silencing of dedifferentiation-related genes. The Journal of neuroscience : the official journal of the Society for Neuroscience. 2011;31(48):17358-69. doi: 10.1523/JNEUROSCI.3931-11.2011. PubMed PMID: 22131398; PubMed Central PMCID: PMC3388739.

62.   Chen ZL, Strickland S. Laminin gamma1 is critical for Schwann cell differentiation, axon myelination, and regeneration in the peripheral nerve. The Journal of cell biology. 2003;163(4):889-99. doi: 10.1083/jcb.200307068. PubMed PMID: 14638863; PubMed Central PMCID: PMC2173689.

63.   Oudega M, Hagg T. Nerve growth factor promotes regeneration of sensory axons into adult rat spinal cord. Experimental neurology. 1996;140(2):218-29. doi: 10.1006/exnr.1996.0131. PubMed PMID: 8690064.

64.   Bunge MB. Bridging areas of injury in the spinal cord. Neuroscientist. 2001;7(4):325-39. PubMed PMID: 11488398.

65.   Hadlock T, Sundback C, Hunter D, Cheney M, Vacanti JP. A polymer foam conduit seeded with Schwann cells promotes guided peripheral nerve regeneration. Tissue Eng. 2000;6(2):119-27. doi: 10.1089/107632700320748. PubMed PMID: 10941207.

66.   Lemons ML, Condic ML. Combined integrin activation and intracellular cAMP cause Rho GTPase dependent growth cone collapse on laminin-1. Experimental neurology. 2006;202(2):324-35. doi: 10.1016/j.expneurol.2006.06.008. PubMed PMID: 16899244.

67.   Nandoe Tewarie RD, Hurtado A, Ritfeld GJ, Rahiem ST, Wendell DF, Barroso MM, et al. Bone marrow stromal cells elicit tissue sparing after acute but not delayed transplantation into the contused adult rat thoracic spinal cord. Journal of neurotrauma. 2009;26(12):2313-22. doi: 10.1089/neu.2009.0987. PubMed PMID: 19645530.

68.   Ritfeld GJ, Tewarie RN, Vajn K, Rahiem ST, Hurtado A, Wendell DF, et al. Bone marrow stromal cell-mediated tissue sparing enhances functional repair after spinal cord contusion in adult rats. Cell Transplant. 2012. doi: 10.3727/096368912X640484. PubMed PMID: 22526408.

69.   Scheff SW, Rabchevsky AG, Fugaccia I, Main JA, Lumpp JE, Jr. Experimental modeling of spinal cord injury: characterization of a force-defined injury device. Journal of neurotrauma. 2003;20(2):179-93. doi: 10.1089/08977150360547099. PubMed PMID: 12675971.

70.   Basso D, Beattie, MS, & Bresnahan, JC. A sensitive and reliable locomotor rating scale for open field testing in rats. Journal of neurotrauma. 1995;12:1-21.

71.   Basso DM, Beattie MS, Bresnahan JC. Graded histological and locomotor outcomes after spinal cord contusion using the NYU weight-drop device versus transection. Experimental neurology. 1996;139(2):244-56. doi: 10.1006/exnr.1996.0098. PubMed PMID: 8654527.

72.   Hargreaves K, Dubner R, Brown F, Flores C, Joris J. A new and sensitive method for measuring thermal nociception in cutaneous hyperalgesia. Pain. 1988;32(1):77-88. PubMed PMID: 3340425.

73.   Ma J, Wu R, Zhang Q, Wu JB, Lou J, Zheng Z, et al. DJ-1 interacts with RACK1 and protects neurons from oxidative-stress-induced apoptosis. The Biochemical journal. 2014;462(3):489-97. doi: 10.1042/BJ20140235. PubMed PMID: 24947010.